

# A STUDY OF THE BRIGHTNESS VARIATIONS IN THE RED SUPERGIANT BC CYGNI

by

Mina Rohanizadegan

A Thesis Submitted to  
Saint Mary's University, Halifax, Nova Scotia  
in Partial Fulfillment of the Requirements for  
the Degree of Masters of Science in Astronomy

August 2006, Halifax, Nova Scotia

© Mina Rohanizadegan, 2006

Supervisor: Dr. David G. Turner,  
Saint Mary's University

Examining Committee:  
Dr. Gary A. Welch,  
Saint Mary's University  
Dr. C. Ian Short,  
Saint Mary's University

External Reviewer:  
Dr. John R. Percy,  
University of Toronto



Library and  
Archives Canada

Bibliothèque et  
Archives Canada

Published Heritage  
Branch

Direction du  
Patrimoine de l'édition

395 Wellington Street  
Ottawa ON K1A 0N4  
Canada

395, rue Wellington  
Ottawa ON K1A 0N4  
Canada

*Your file* *Votre référence*  
*ISBN: 978-0-494-25522-3*  
*Our file* *Notre référence*  
*ISBN: 978-0-494-25522-3*

**NOTICE:**

The author has granted a non-exclusive license allowing Library and Archives Canada to reproduce, publish, archive, preserve, conserve, communicate to the public by telecommunication or on the Internet, loan, distribute and sell theses worldwide, for commercial or non-commercial purposes, in microform, paper, electronic and/or any other formats.

The author retains copyright ownership and moral rights in this thesis. Neither the thesis nor substantial extracts from it may be printed or otherwise reproduced without the author's permission.

**AVIS:**

L'auteur a accordé une licence non exclusive permettant à la Bibliothèque et Archives Canada de reproduire, publier, archiver, sauvegarder, conserver, transmettre au public par télécommunication ou par l'Internet, prêter, distribuer et vendre des thèses partout dans le monde, à des fins commerciales ou autres, sur support microforme, papier, électronique et/ou autres formats.

L'auteur conserve la propriété du droit d'auteur et des droits moraux qui protègent cette thèse. Ni la thèse ni des extraits substantiels de celle-ci ne doivent être imprimés ou autrement reproduits sans son autorisation.

---

In compliance with the Canadian Privacy Act some supporting forms may have been removed from this thesis.

Conformément à la loi canadienne sur la protection de la vie privée, quelques formulaires secondaires ont été enlevés de cette thèse.

While these forms may be included in the document page count, their removal does not represent any loss of content from the thesis.

Bien que ces formulaires aient inclus dans la pagination, il n'y aura aucun contenu manquant.

  
**Canada**

---

# Abstract

## A STUDY OF THE BRIGHTNESS VARIATIONS IN THE RED SUPERGIANT BC CYGNI

By Mina Rohanizadegan

The variability of the type C semi-regular (SRC) M3.5 Ia supergiant variable BC Cyg is examined with reference to measurements of its photographic  $B$  magnitude derived from 866 archival plates in the Harvard and Sternberg collections as well as eye estimates of its visual  $V$  magnitude made by members of the AAVSO. BC Cyg is the brightest member of the young open cluster Berkeley 87, so it has a well established reddening, distance, and age. A discrete Fourier analysis was performed on the BC Cygni light curve, as well as on individual subsets of the data. The analysis was made to study the fundamental periods of variability in this red supergiant variable. BC Cyg exhibits interesting features in its century-long baseline of brightness variations that relate to fundamental mode envelope pulsation as well as evolution: an  $0^m.5$  increase in  $\langle B \rangle$  over the past century in conjunction with a steady decrease in pulsation period from  $\sim 697^d$  in 1900 to  $688^d$  in 2000. Despite the increase in  $\langle B \rangle$ , the star's luminosity appears to have decreased over the past century, presumably as a result of stellar evolutionary effects. A detailed examination of a well sampled portion of the star's light curve, data spanning the interval HJD 2442000 to 2449000, by means of non-linear least squares analysis indicates that only one periodicity (686 days) exists in the observations. No secondary periodicity can be detected, to within the constraints of observational uncertainty.

Date: August 2006

# Acknowledgements

I acknowledge with thanks the variable star observations from the AAVSO International Database contributed by observers worldwide and used in this research. I also thank my supervisor, Dr. David Turner, who read my numerous revisions and for his guidance and support. I am also grateful to my committee members, Dr. Gary Welch, Dr. Ian Short, and Dr. John R. Percy, for reading this thesis and making helpful suggestions for improvement.

# Contents

<b>Abstract</b> . . . . .	ii
<b>Acknowledgements</b> . . . . .	iii
<b>Contents</b> . . . . .	iv
<b>List of Figures</b> . . . . .	vi
<b>List of Tables</b> . . . . .	ix
<b>1 Introduction</b> . . . . .	1
1.1 Type C Supergiant Semiregular Variable Stars . . . . .	1
1.2 Background on the program star . . . . .	4
<b>2 Data Acquisition and Preliminary Reduction</b> . . . . .	6
2.1 Data Collection . . . . .	6
2.2 Amplitude Variation with Brightness in SRC variables . . . . .	13
2.3 Fourier Analysis and the Fourier Transform . . . . .	17
2.4 Power Spectrum Analysis . . . . .	17
2.5 Evolution of the main periodicity . . . . .	19
2.6 Uncertainties In Period Determinations . . . . .	22
2.7 Period Estimates for a Few Other SRC Variables . . . . .	25
2.8 Non-linear Least Squares Fitting . . . . .	35
<b>3 The Period Searches and Their Results</b> . . . . .	36

---

<b>4</b>	<b>Implication of the Results</b> . . . . .	42
4.1	Brightness Variation . . . . .	42
4.2	Characteristics of the Light Curve . . . . .	48
<b>5</b>	<b>Summary</b> . . . . .	49
<b>6</b>	<b>Appendix</b> . . . . .	51
<b>7</b>	<b>Bibliography</b> . . . . .	67

# List of Figures

1.1	An image of the sky centred on BC Cyg, where Berkeley 87 is the cluster of stars lying at the bottom of the image. North is toward the top of the image, and east is toward the left hand side of the image. . . . .	5
2.1	What we observe for a black-body at a temprature of 5000K, where the spectral peak, $\lambda_s$ , falls to the redward side of the peak wavelength for the filter, $\lambda_p$ . The effective wavelength for the filter/spectrum combination is $\lambda_e$ , redward of $\lambda_p$ . . . . .	8
2.2	Nearly contemporaneous data for the Harvard (y-axis) and Sternberg (x-axis) data sets. The least squares fit shown is described by: $B(\text{Harvard}) = 4.172 + 0.672 B(\text{Sternberg})$ . . . . .	9
2.3	The light curve of BC Cyg in the $B$ band from the full data set. . . . .	10
2.4	The $B$ band light curve of BC Cyg at an expanded temporal scale. . . . .	11
2.5	The visual light curve of BC Cyg, data courtesy of the AAVSO international database (Henden 2006). . . . .	12
2.6	The light curve of the SRC variable VX Sgr in the $V$ band, data courtesy of the AAVSO international database (Henden 2006). . . . .	14
2.7	The light curve of the SRC variable W Tri in the $V$ band, data courtesy of the AAVSO international database (Henden 2006). . . . .	15
2.8	The light curve of the SRC variable AH Sco in the $V$ band, data courtesy of the AAVSO international database (Henden 2006). . . . .	16
2.9	A power spectrum showing how power varies with frequency for the complete sample of $B$ band data for BC Cyg. . . . .	19

---

2.10	The period of BC Cyg decreased from 700 to 688 days over the interval spanned by the observations. A least squares fit was made to the data, which is illustrated along with the estimated uncertainties. . . . .	20
2.11	The evolution of the average brightness of BC Cyg as derived from running 50-day means of the original data sample. A trend line was fitted to the data by means of a least squares analysis. . . . .	21
2.12	A sample power spectrum of the envelope around the period peak. . . . .	23
2.13	The light curve of the SRC variable AD Per in the <i>V</i> band, data courtesy of the AAVSO international database (Henden 2006). . . . .	26
2.14	The power spectrum of AD Per. . . . .	26
2.15	The light curve of the SRC variable RS Per in the <i>V</i> band, data courtesy of the AAVSO international database (Henden 2006). . . . .	27
2.16	The power spectrum of RS Per. . . . .	27
2.17	The light curve of the SRC variable S Per in the <i>V</i> band, data courtesy of the AAVSO international database (Henden 2006). . . . .	28
2.18	The power spectrum of S Per. . . . .	28
2.19	The light curve of the SRC variable SU Per in the <i>V</i> band, data courtesy of the AAVSO international database (Henden 2006). . . . .	29
2.20	The power spectrum of SU Per. . . . .	29
2.21	The light curve of the SRC variable YZ Per in the <i>V</i> band, data courtesy of the AAVSO international database (Henden 2006). . . . .	30
2.22	The power spectrum of YZ Per. . . . .	30
2.23	The light curve of the SRC variable Alpha Her in the <i>V</i> band, data courtesy of the AAVSO international database (Henden 2006). . . . .	31
2.24	The power spectrum of Alpha Her. . . . .	31

2.25	The light curve of the SRC variable T Cet in the $V$ band, data courtesy of the AAVSO international database (Henden 2006). . . . .	32
2.26	The power spectrum of T Cet. . . . .	32
2.27	The power spectrum of VX Sgr. . . . .	33
2.28	The power spectrum of W Tri. . . . .	33
2.29	The power spectrum of AH Sco. . . . .	34
3.1	The selected part of the light curve of BC Cyg. . . . .	38
3.2	Power spectrum of the original data spanning from HJD 2442000 to 2449000. . . . .	38
3.3	Power spectrum of the original data after prewhitening with a fitted sine function of the form: $B = A_1 \sin((2.0\pi hjd/P_1) + \Phi_1) + \bar{n}$ . . . . .	39
3.4	A plot of Fourier amplitude versus frequency of the residual data (original - $P_1$ ) . . . . .	39
3.5	Residuals in the light curve of BC Cyg after fitting the data using a single period $P_1$ . . . . .	40
3.6	Light curve of BC Cyg with the main frequency fitted on it. . . . .	41
4.1	A finding chart for Berkeley 87, as derived from the POSS E-plate of the region. North is toward the top of the image, and east is toward the left hand side of the image. . . . .	44
4.2	The observed colours of BC Cyg as a function of the stars's photographic magnitude as derived from averages of AAVSO visual estimates combined with photographic estimates of the star made within roughly ten days of each other. . . . .	45
4.3	A theoretical H-R diagram showing evolutionary tracks for stars of $9M_\odot$ , $15M_\odot$ , and $20M_\odot$ and $Z = 0.02$ (Schaller et al. 1992), and the estimated parameters for BC Cyg over its pulsation cycle around 1900 (filled circles) and 2000 (open diamonds). . . . .	46
4.4	A period-luminosity relation for SRC variables in Per OB1 (filled circles) and BC Cyg (star) constructed from $BV$ data for the stars. Shown for comparison is a theoretical pulsation model for Galactic red supergiants with $Z = 0.02$ (solid line) from Guo and Li (2002). . . . .	47

# List of Tables

2.1	A summary of the data for the frequency with the highest power and period peak, the corresponding power and sigma, number of data points used in the fit, $\langle \text{HJD} \rangle$ , and the duration of each interval in the sample. . . . .	24
2.2	A summary of the peak period for the above SRC variables. . . . .	34
6.1	Estimated values for BC Cyg at its faintest and brightest . . . . .	52
6.2	Blue band data from the collection of the Sternberg Observatory . . . . .	53
6.3	Blue estimates from Harvard College Observatory plus converted blue band data from Sternberg Observatory. . . . .	55
6.4	Visual observations from the AAVSO . . . . .	62
6.5	Photographic visual estimates collected by the author at Harvard Observatory . . . .	66

---

# Chapter 1

## Introduction

### 1.1 Type C Supergiant Semiregular Variable Stars

Red supergiants are the largest stars known, with dimensions that can exceed the orbit of the planet Mars in our solar system. They are also very luminous, although with an upper limit near  $M_{\text{Bol}} \simeq -9.5$  (Humphreys 1987) they are still less luminous than hot blue hypergiants found in many spiral galaxies. Even with that restriction, they can still radiate almost a million times more light than the Sun.

Cool M-type supergiants are fairly rare massive stars that display the physical properties of highly evolved objects with progenitor masses of less than about  $20M_{\odot}$  according to stellar evolutionary models by Meynet et al. (1993), in which mass loss was considered without any assumption about rotation. The upper luminosity limit for such stars is restricted by radiation pressure to the Eddington limit and explains the fact that more massive stars cannot evolve into the red supergiant region, but remain as hotter stars until their eventual explosion as Type II supernovae (Chevalier 1981). The upper limit to red supergiant masses and luminosities is a recognizable feature in the H-R diagrams for luminous stars in other galaxies (Humphreys 1987).

Photometric monitoring, the regular collection of light in various pass bands, of M supergiants over the past century demonstrates that their light output tends to be fairly periodic, yet with distinct non-periodic trends with time. Most are described as semi-regular, which, according to Hoffmeister et al. (1985), means that their periodic trends change with time so that maxima and minima cannot always be determined, even if regular periodic cycles are later re-established. The average quasi-period of a supergiant can be anywhere from a few hundred to several hundred days

---

in duration, depending upon the physical parameters of its atmosphere (mainly the mean density, temperature gradients, etc.). The periodicity is usually ascribed to vertical displacements of patches on the stellar surface or to the motion of the complete stellar surface, which astrophysicists describe as envelope pulsation. The rather irregular behavior of red supergiants indicates that their surface motions may behave in a rather incoherent fashion. In some cases the Fourier analysis of temporal groupings of data can reveal the existence of smaller amplitude periodicities in the light curve data. They may be the result of large-scale motions in the extended atmospheres, the rotation of starspots across the visible hemisphere, or starspot cycles, but one must always be careful to establish that they are not simply aliases of other cycles occurring in the data.

Sharpless et al. (1966) found that most M supergiants are located in or near OB associations, primarily in the Galactic plane. Because of their high luminosity, they can be observed to very great distances, particularly in the infrared where the effects of interstellar extinction are reduced. Since supergiants are stars of extreme Population I, they are very important for studying Galactic structure.

The long period variables that include M supergiants as members fall into distinct groups, both from an observational and evolutionary view point. Mira variables are red giant variables that pulsate with large amplitude, and have masses of only a few times the Sun's mass. Closely related to Miras are the semi-regular variables of types A and B, SRA and SRB, that are also red giants but which display smaller amplitude variations. They too have masses close to that of the Sun. Type C semi-regular variables, SRC, constitute a separate category of stars that include only red supergiant variables of spectral type M or their chemically peculiar equivalents. All are massive stars ( $\leq 20M_{\odot}$ ) burning helium or carbon in or around a non-degenerate core. Members of the class typically have more irregular light curves than Miras, and have a wider range of light amplitudes.

The type C semi-regular variables, SRC, constitute a small group of 55 stars in the *General Catalogue of Variable Stars* (GCVS; Kholopov et al. 1985) that, in contrast to the SRA and SRB variables, include some of the most massive and exotic stars in the Milky Way. A prime example is

---

Betelgeuse ( $\alpha$  Orionis, spectral type M1-2 Ia-Iab), whose light variations have been followed since the early 1800s. The origin of variability in such stars is not fully understood, although, as mentioned above, pulsation and the rotation of bright or dark spots across the visible hemisphere are believed to play an important role. The brightness variations in some of the stars display abrupt changes in their mean values, which may be tied to evolution near the red supergiant tip.

Because SRC variables have very long cycles, long time spans of data are necessary to reveal their pulsation characteristics. In fact, considerable amounts of observing time are necessary to establish accurately the length of a given star's pulsational cycle. Unfortunately, insufficient data or data that include large temporal gaps can yield misleading results for the derived period.

This study presents and analyzes extensive photometric data for a specific Type C semi-regular variable, BC Cygni, as a possible prototype of the class. Long period variables (LPVs) have generated interest as possible distance indicators. According to Pierce et al. (2000) and Jurcevic et al. (2000), long period variables, and SRCs in particular, are much more common than Cepheids in spiral galaxies, are more luminous than Cepheids, and also obey a period-luminosity relation of their own that makes them inherently valuable distance indicators. They are therefore potentially valuable standard candles for the distance scale to nearby galaxies. The problem is that red supergiants tend to be relatively little studied and less well understood than their yellow supergiant kin.

One of the great discoveries in modern astronomy was made by Henrietta Leavitt in 1912, who found that the apparent magnitude of Cepheids in the Small Magellanic Cloud decreased with increasing period, a feature now recognized as the period-luminosity, or P-L relation. Long period variable stars (LPVs) also exhibit a period-luminosity relation that can be used to determine distances to stellar systems containing significant LPV populations (Feast 1984, Wood and Bessell 1985). Distance moduli obtained from the LPV period-luminosity relation are independent of other methods that have previously been used to determine distances to external galaxies. For instance, Pierce et al. (2000) have established a P-L relation for Galactic SRCs from studies of M supergiants in Per OB1, and used the results to establish distances to M33 and M101 from  $R$  and  $I$  pass band

photometry of LPVs in the galaxies (Jurcevic et al. 2000). Glass (1979) found that SRC variables in the Large and Small Magellanic Clouds also follow a PL relation, which was confirmed using data for additional LMC SRC variables by Feast et al. (1980).

Stothers (1969b) used stellar evolutionary models with convective envelopes in adiabatic equilibrium, including radiation pressure, to confirm pulsation as the likely origin of variability in M supergiants, at the same time noting the existence of a period-luminosity relation for cluster and association members. A different treatment by Li and Gong (1994) that includes both non-adiabatic effects and the coupling between convection and pulsation also provides a theoretical period-luminosity relation for M supergiant variables. Such a tool can be used to reveal stellar properties when compared with existing observational counterparts, and can provide valuable information about stellar interiors through pulsation theory.

## 1.2 Background on the program star

BC Cygni is a cool, red supergiant that displays semiregular variability. It is listed in the *General Catalogue of Variable Stars* (GCVS; Kholopov et al. 1985) as a SRC variable with a spectral classification of M3.5 Ia, displaying moderate amplitude variability. More importantly, it is located near the edge of the young cluster Berkeley 87 (= Dolidze 7 = C2019+372,  $\ell = 75^\circ.71$ ,  $b = +0^\circ.31$ ), lying in a heavily-obscured region of Cygnus (Turner and Forbes 1982), and is almost certainly a cluster member. Because of the likely cluster membership of BC Cyg, its age ( $\sim 10^7$  years) and original mass ( $\sim 20M_\odot$ ) are known reasonably well.

BC Cyg is one of the more luminous M supergiants, given that it is of luminosity class Ia, so is more likely to turn into a Type II supernova sooner than many other, less luminous, and hence less massive, members of the class. A major obstacle to a full understanding of the physical mechanism(s) responsible for the light variations in such stars is often the lack of temporal data on their brightness changes, which tend to be repeatable, or nearly repeatable, over time scales of several hundreds to

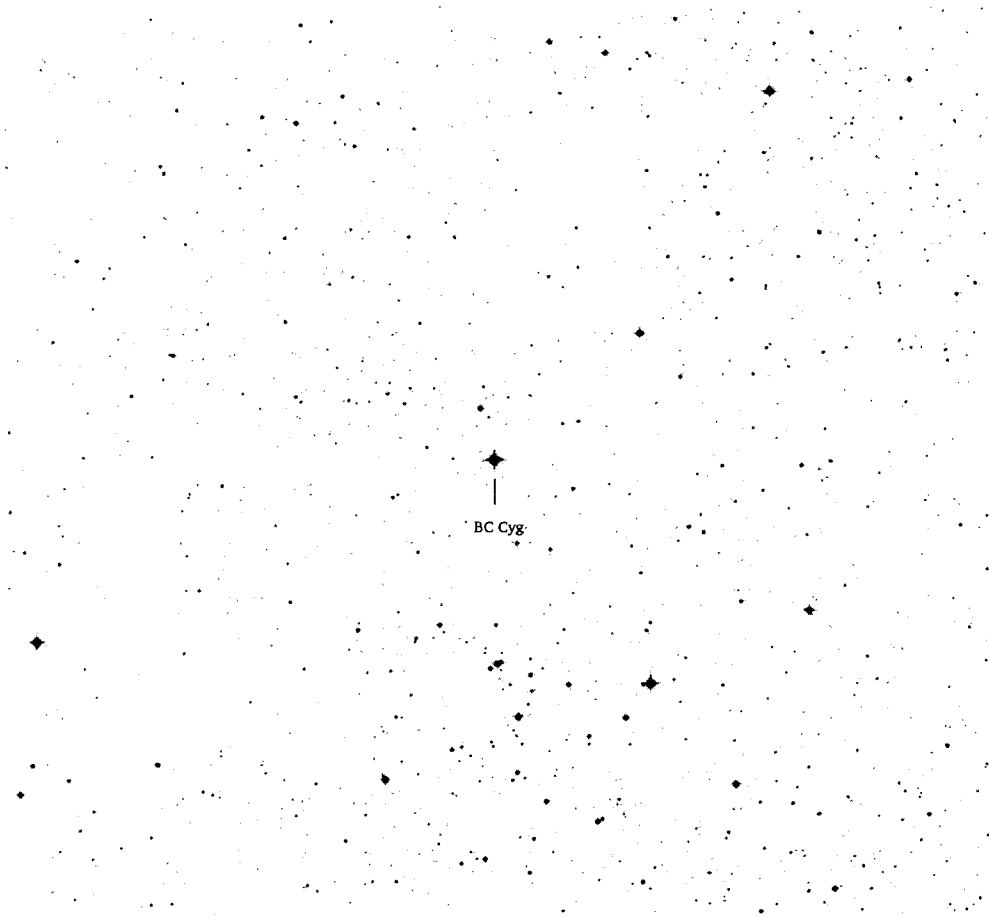


Figure 1.1: An image of the sky centred on BC Cyg, where Berkeley 87 is the cluster of stars lying at the bottom of the image. North is toward the top of the image, and east is toward the left hand side of the image.

thousands of days or more. To that end we have managed to collect a fairly extensive database of brightness variations in BC Cyg that provides some clues on what may be responsible for its variability. Figure 1.1 shows the region of sky that contains BC Cyg. The image is from the STScI Digital Sky Survey, and measures 30 arcmin by 30 arcmin.

## Chapter 2

# Data Acquisition and Preliminary Reduction

### 2.1 Data Collection

An extensive set of brightness data for BC Cyg was constructed from eye estimates of its photographic ( $B$ ) magnitude, relative to a reference sequence of stars in Berkeley 87 observed photoelectrically, obtained from plates in the collection of the Sternberg Astronomical Institute by Elena N. Pastukhova and Leonid N. Berdnikov during Fall 2004, as well as from patrol series plates in the Harvard College Observatory Photographic Plate Collection obtained by David G. Turner during Summer 2002, Fall 2004, and Spring 2005. The vast majority of observations in the data set come from plates in the Harvard collection.

The astronomical collection at the Harvard College Observatory consists of more than a half million photographic plates taken between the mid 1880s and 1995 (with a gap between 1953-68). The majority are direct blue plates taken with a variety of refractors, and have focal scales ranging from 60 to 600 arcsec/mm. Magnitude estimates for BC Cyg were made by comparing its image size and darkness to similar images of nearby reference stars surrounding it, by the usual method of visual step interpolation and comparison employed for centuries by variable star observers. The brightness of BC Cyg on all plates is a few magnitudes above the plate limits, in a region of the characteristic curve for the emulsions which is most sensitive to small changes in brightness. The magnitude estimates for BC Cyg are therefore generally accurate to about  $\pm 0.1$ , and probably not larger than  $\pm 0.2$ . In some cases, such as for plates in the high resolution series rather than the patrol series, the estimated uncertainties seem likely to be smaller than  $\pm 0.1$ .

The blue magnitude estimates for BC Cyg range from 12.0 to 13.4, as illustrated in Figures 2.3 and 2.4, and the interval of the observations spans just over a century, from Julian dates 2413452 to 2450284. The AAVSO international database visual estimates for BC Cyg range from 8.4 to 11.4 and spread over a time span from JD 2433264 to JD 2448458. The data used in making estimates for  $B$  and  $V$  are summarized in Tables 6.2, 6.3, and 6.4 of the Appendix.

More recent additions to the Harvard collection include photographic visual ( $V$ ) plates in the Damon series. Most are contemporaneous with  $B$  plates in the same series. Magnitude estimates were made from the plates by the author, and are presented in Table 6.5 of the Appendix, but the values were found to be brighter than eye estimates made by AAVSO observers. It appears that the telescope/filter/emulsion combination for the Harvard  $V$  plates overestimates the brightness of red stars, so the data listed in Table 6.5 proved to be unsuitable for inclusion in the study. In order to obtain the  $V$  magnitude estimates, a number of reference stars around BC Cyg were identified, their magnitudes being obtained from sources in the VizieR data bases, Hipparcos measurements mainly. The next step was to estimate BC Cyg's magnitude on individual plates by comparing the size and intensity of the image to the nearby reference sequence. The magnifier used for that purpose was of low power, roughly 5 to 10 power, and typical uncertainties were estimated to be about  $\pm 0.1$  to  $\pm 0.2$ , as above. All of the plates in the Damon series are of excellent quality and resolution, much more so than patrol series plates in the Harvard collection.

Note that Table 6.2 of the Appendix contains the combined Harvard and Sternberg Observatory data sets. With regard to the Sternberg data, a transformation was necessary to account for the different emulsion/filter systems employed at the Sternberg Observatory relative to those used at Harvard sites. When we observe a star through a particular filter, the signal we measure is a convolution of the pass band with the stellar spectrum, as in Figure 2.1. If a cool star is observed photometrically, the spectral energy distribution for the star has a peak ( $\lambda_s$ ) that falls to the redward side of the peak wavelength for the filter,  $\lambda_p$ . What is measured is the convolved flux, which has a maximum near  $\lambda_e$ , redward of the peak wavelength sensitivity for the filter. A different tele-

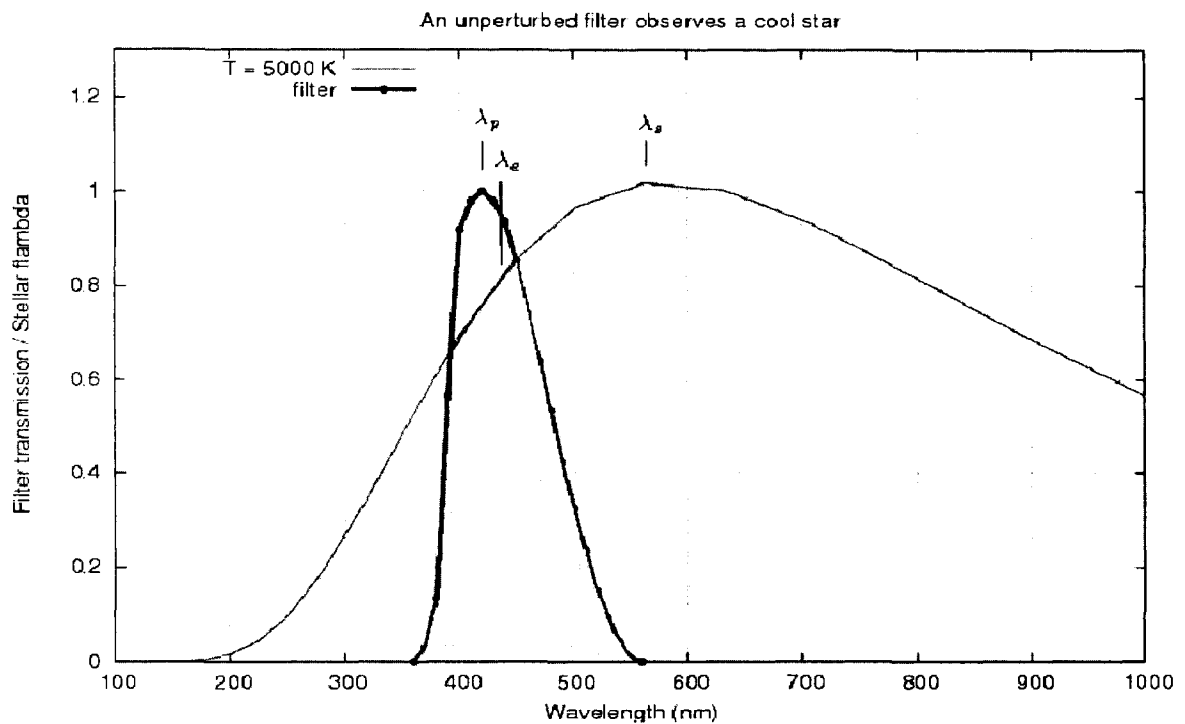


Figure 2.1: What we observe for a black-body at a temperature of 5000K, where the spectral peak,  $\lambda_s$ , falls to the redward side of the peak wavelength for the filter,  $\lambda_p$ . The effective wavelength for the filter/spectrum combination is  $\lambda_e$ , redward of  $\lambda_p$ .

scope/filter/emulsion combination will sample a different portion of the spectral energy distribution for the star, and can result in a different total brightness for the star in the same filter band for observations made on the same date. There appear to be slight differences between the sensitivities of the filter/telescope/*B* emulsion combinations used at Sternberg and Harvard Observatories, as seen in Figure 2.2, which plots Harvard *B* magnitudes as a function of Sternberg *B* magnitudes for nearly contemporaneous observations from the two sites. It was therefore necessary to correct observations from Sternberg and Harvard to the same scale. That was done using the relationship obtained from a least squares fit to the data of Figure 2.2, which should adjust values for  $B(\text{Sternberg})$  to their equivalent values in the  $B(\text{Harvard})$  system.

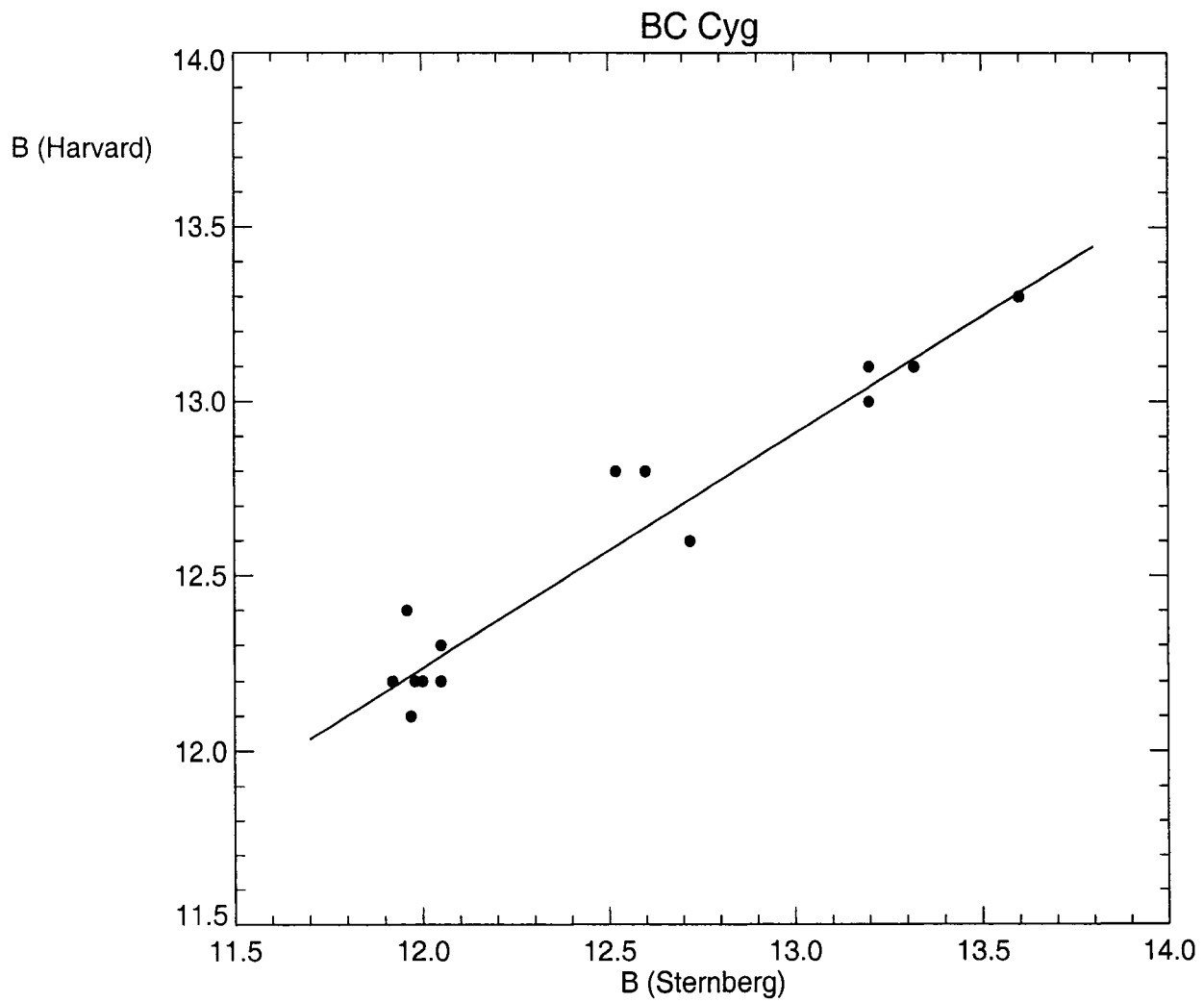


Figure 2.2: Nearly contemporaneous data for the Harvard (y-axis) and Sternberg (x-axis) data sets. The least squares fit shown is described by:  $B(\text{Harvard}) = 4.172 + 0.672 B(\text{Sternberg})$ .

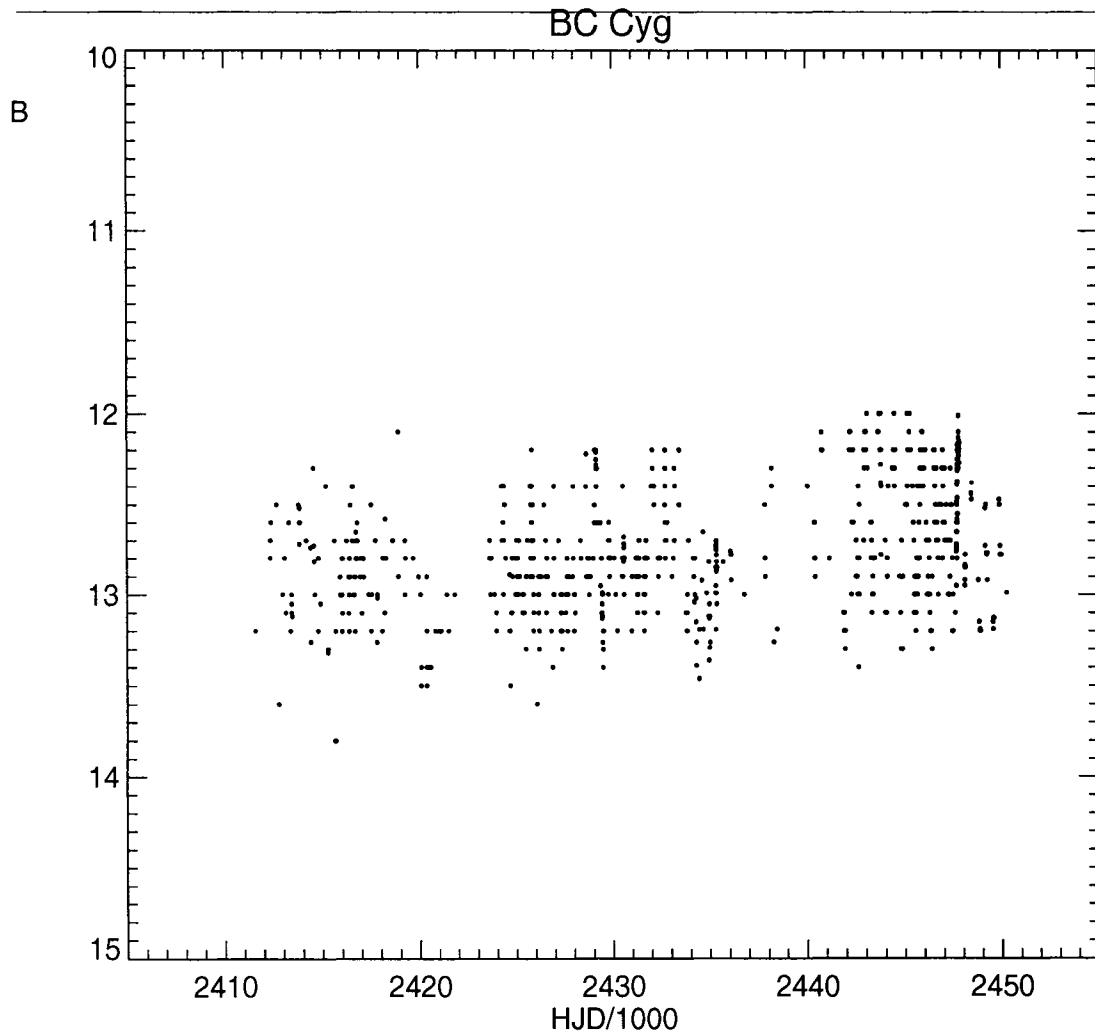


Figure 2.3: The light curve of BC Cyg in the  $B$  band from the full data set.

Figure 2.3 shows the resulting  $B$  band data for BC Cyg from a combination of Harvard and Sternberg plate estimates, while Figure 2.4 illustrates the same data on an expanded temporal scale to illustrate the main periodicity of the star. Figure 2.5 shows similar  $V$  data for the star, as obtained from the international database of the American Association of Variable Star Observers (AAVSO) (Henden 2006).

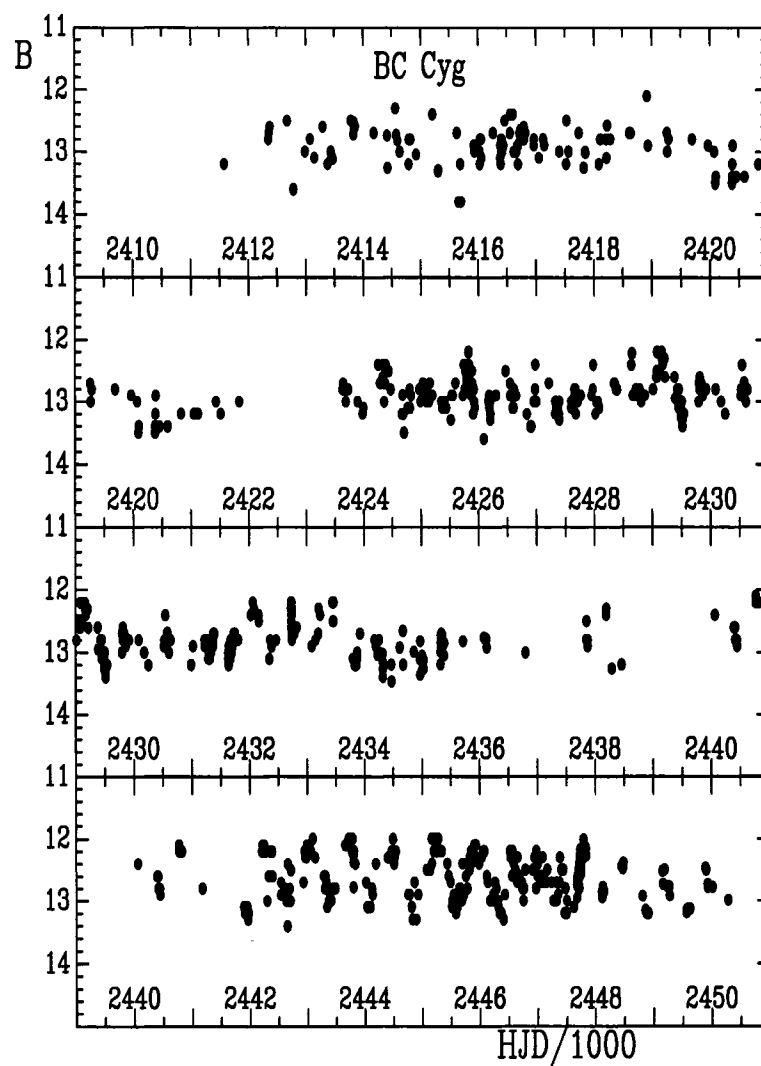


Figure 2.4: The  $B$  band light curve of BC Cyg at an expanded temporal scale.

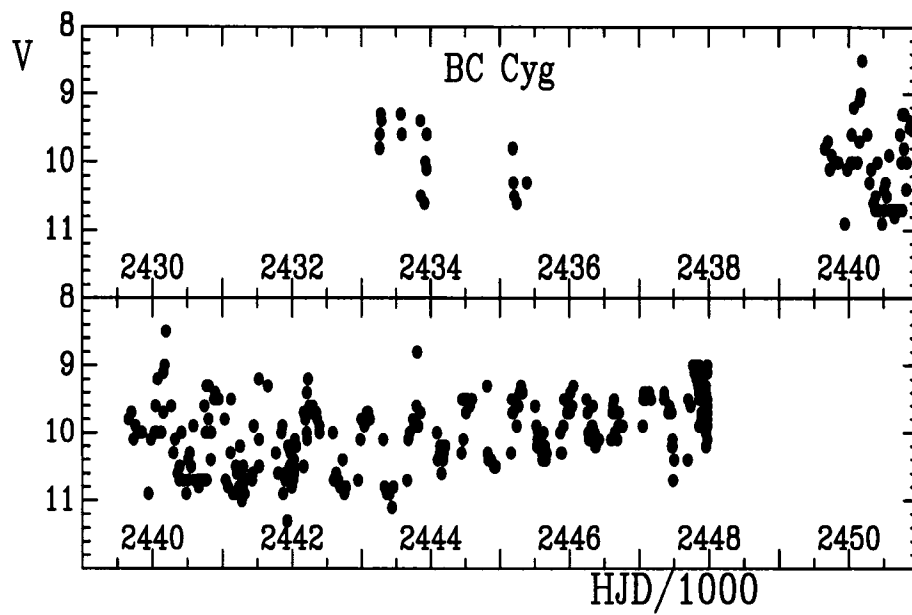


Figure 2.5: The visual light curve of BC Cyg, data courtesy of the AAVSO international database (Henden 2006).

## 2.2 Amplitude Variation with Brightness in SRC variables

Amplitude modulation in pulsating variables is mainly associated with RR Lyrae variables, with  $\delta$  Scuti stars that have very complex light variations (e.g., Breger 1993; Mantegazza et al. 1996), and with some Mira and semi-regular variables (Barthes and Mattei 1997; Mattei 1993; Mattei et al. 1997; Mattei and Foster 2000). The underlying physical cause is unknown, although several possible mechanisms are suspected, such as rotation of star spots across the visible hemisphere, magnetic activity cycles comparable to the sunspot cycle, or duplicity effects arising from companions (Kiss et al. 1999). The characteristic time scales for amplitude modulation in such stars are around 4000 days, close to the typical theoretically calculated rate of rotation for red giant stars, as estimated from rotational velocities by Schrijver and Pols (1993) and Kiss et al. (1999).

Figures 2.6, 2.7, and 2.8 demonstrate typical examples of light curves for three SRC variables that display temporal variations in light amplitude. Both amplitude variations and slow changes in mean light level are seen, in addition to regular cyclical variations. The luminous SRC variable VX Sgr, of spectral type M4 Iae according to Monnier et al. (1998), displays all three features most noticeably.

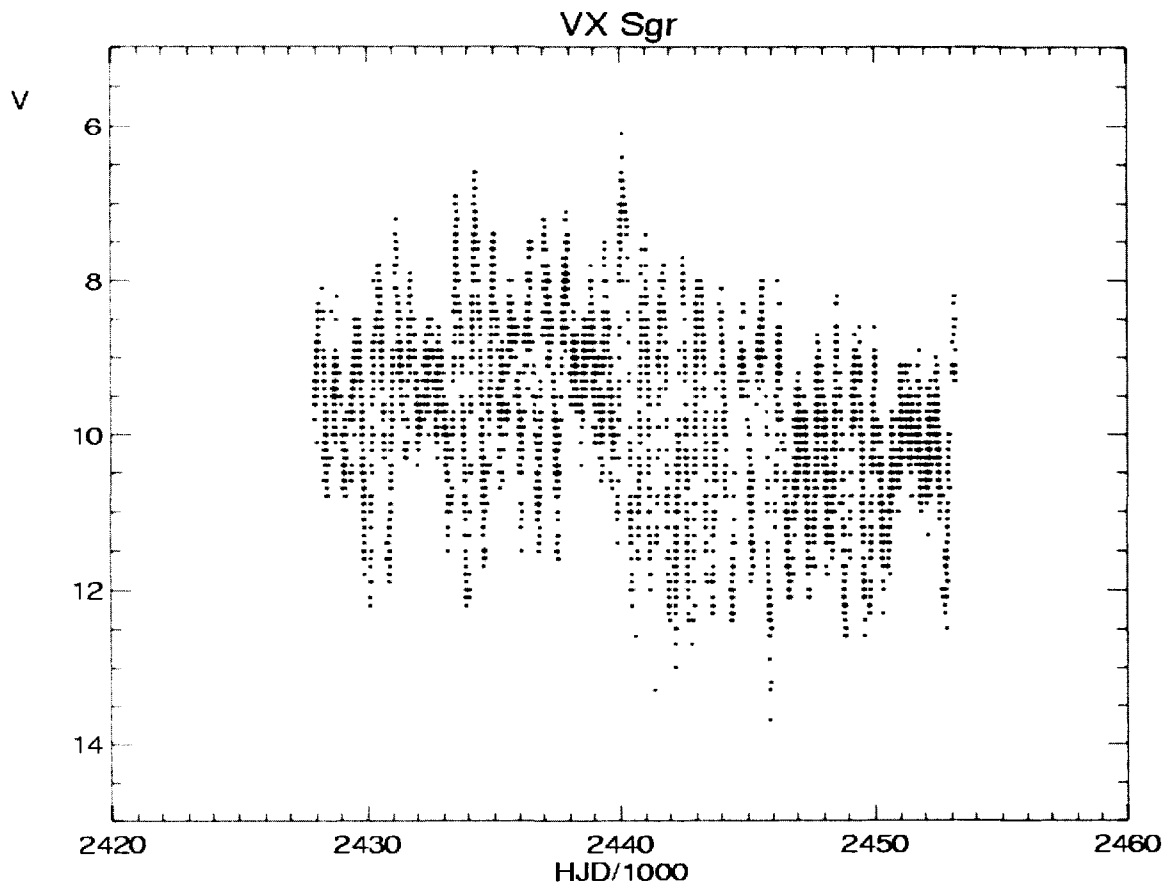


Figure 2.6: The light curve of the SRC variable VX Sgr in the  $V$  band, data courtesy of the AAVSO international database (Henden 2006).

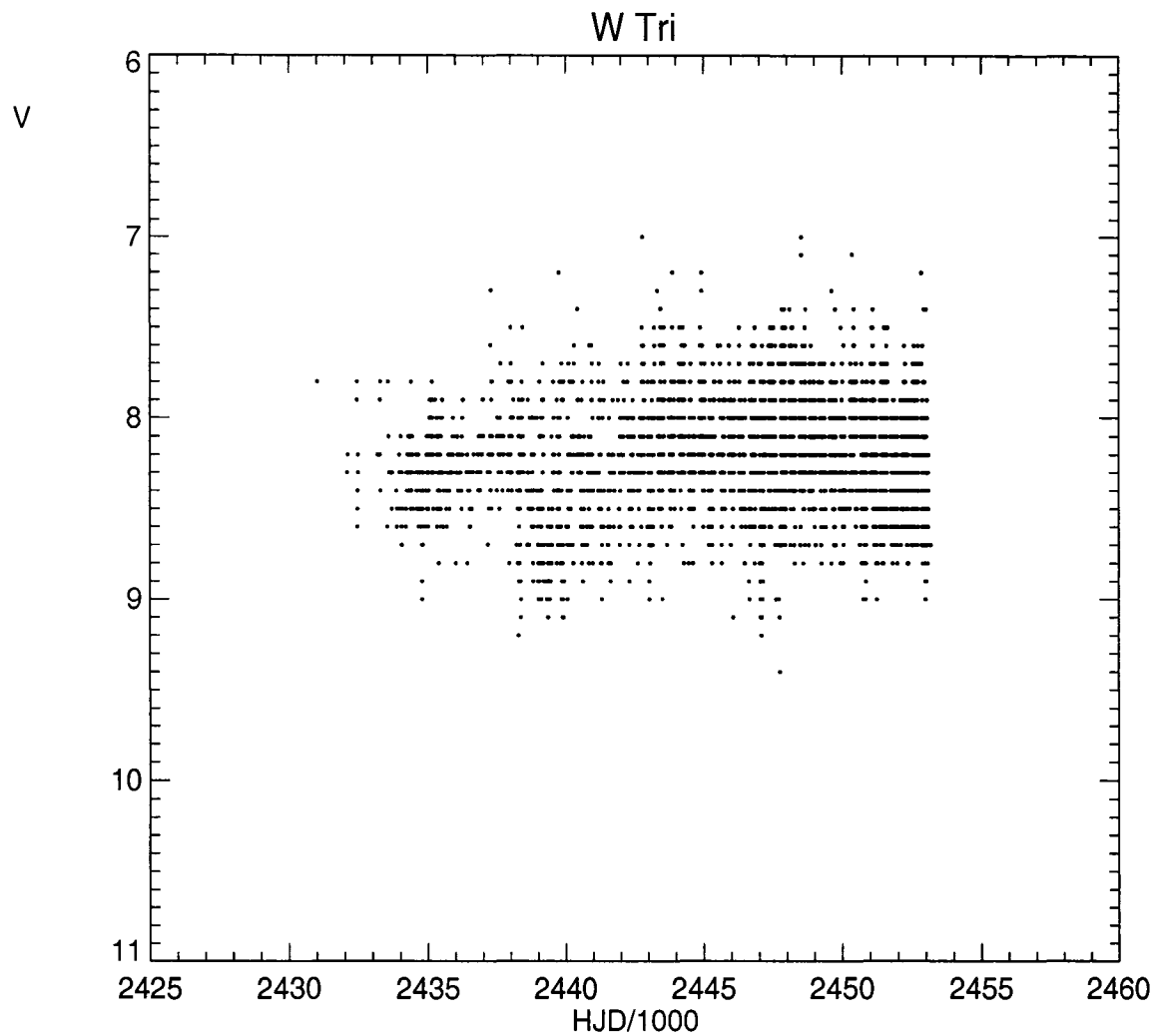


Figure 2.7: The light curve of the SRC variable W Tri in the *V* band, data courtesy of the AAVSO international database (Henden 2006).

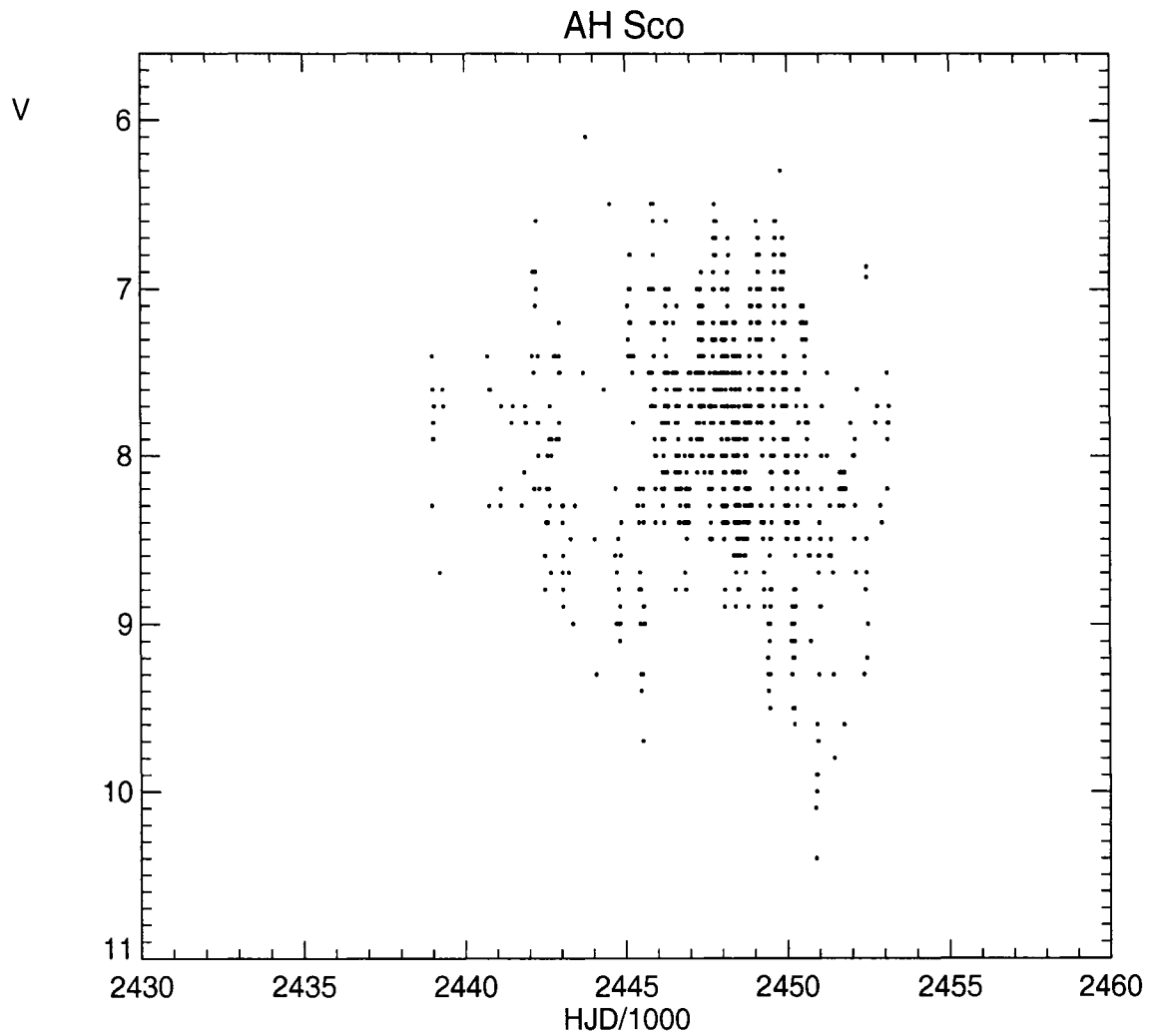


Figure 2.8: The light curve of the SRC variable AH Sco in the  $V$  band, data courtesy of the AAVSO international database (Henden 2006).

## 2.3 Fourier Analysis and the Fourier Transform

Fourier analysis is the technique of using a finite number of sine and cosine functions of different periods, amplitudes, and phases to represent a given set of numerical data or an analytic function. In so doing one can estimate the period (or periods) of variability by determining which functions are statistically significant. The amplitudes (and phases) of the components are determined with a Fourier transform.

If we are presented with a set of time-varying data, given by  $x(t)$ , then the Fourier transform,  $F(\nu)$ , of the data set is given by the integral

$$F(\nu) = \int_{-\infty}^{\infty} x(t) \exp(-i2\pi\nu t) dt, \quad (2.1)$$

where  $\nu$  is the frequency, defined as  $\nu = 1/P$  (where  $P$  is the cyclical period of variability),  $i$  is the square root of  $-1$ , and the sine and cosine functions are represented by the complex exponential function given by Euler's formula:

$$\exp(-i2\pi\nu t) = \cos(-2\pi\nu t) + i \sin(-2\pi\nu t). \quad (2.2)$$

## 2.4 Power Spectrum Analysis

A power spectrum is the distribution of power values as a function of the trial frequency, where "power" is considered to be  $\text{Power}(\nu) = |F(\nu)|^2 = F^*(\nu)F(\nu)$ , so total power =  $\int_{-\infty}^{\infty} |F(\nu)|^2 d\nu$  (Press et al. 1992).

An estimate of the power spectrum of a time series can be obtained by means of a discrete Fourier transform. Suppose that the function  $c(t)$  is sampled at  $N$  points to produce values  $c_0 \dots c_{N-1}$ , and that the points span a range of time  $T$ , that is  $T = (N - 1)\Delta$ , where  $\Delta$  is the sampling interval. Now, if we take an  $N$ -point sample of the function  $c(t)$  at equal intervals and use the FFT (Fast

Fourier Transform) to compute its discrete Fourier transform, then

$$c_k = \sum_{j=0}^{N-1} c_j e^{2\pi i j k / N}, \quad k = 0, 1, \dots, (N-1), \quad (2.3)$$

and the power estimate of the power spectrum is defined at  $\frac{1}{2}N + 1$  frequencies as

$$P(0) = P(\nu_0) = \frac{1}{N^2} |c_0|^2, \quad (2.4)$$

$$P(\nu_k) = \frac{1}{N^2} [|c_k|^2 + |c_{N-k}|^2], \quad k = 1, 2, \dots, (N/2 - 1), \quad (2.5)$$

$$P(\nu_c) = P(\nu_{N/2}) = \frac{1}{N^2} |c_{N/2}|^2. \quad (2.6)$$

Note that the FFT is the same as the discrete Fourier transform, with the difference that a discrete length of  $N$  is rewritten as the sum of two discrete lengths, each of length  $N/2$ . One of the two is formed from the even-numbered points of the original  $N$ , the other from the odd-numbered points.

The software TS (time series, Foster 1996) is a Fourier-searching, FORTRAN based, time-series statistical program designed to analyze variable star data, and is available on-line from the AAVSO website. The software has been used in this thesis to obtain power spectra for BC Cyg. As an example, Figure 2.9 is a power spectrum for the complete sample of data for BC Cyg.

Because of the manner in which astronomical observations are obtained, most data samples contain certain alias signals corresponding to cycle lengths of one or more days, or of one or more years. They are produced by the uncertainty that arises in the number of cycles elapsed during times when the object is not observed. For data sets with such an aliasing effect, one can usually ignore peaks that do not have significant power relative to the highest peak. However, for data containing multiple, closely-spaced periodicities, the interaction of two or more alias envelopes in conjunction with the harmonic phenomenon discussed below can be difficult to sort out.

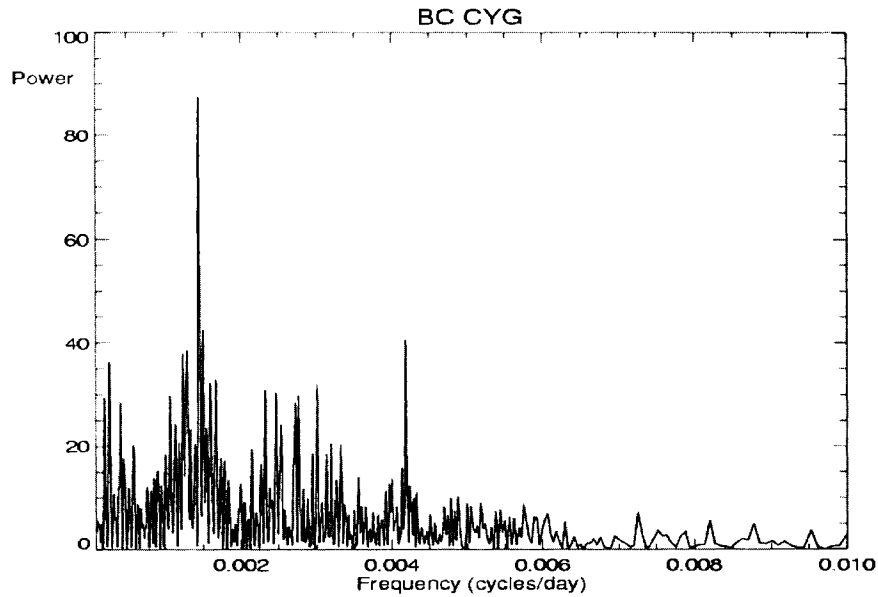


Figure 2.9: A power spectrum showing how power varies with frequency for the complete sample of *B* band data for BC Cyg.

## 2.5 Evolution of the main periodicity

In Figure 2.9 a frequency of 0.001445 cycle per day produces the largest observable power in the data set. That frequency is equivalent to a period of 692 days, and is considered to correspond to the main periodicity of BC Cyg.

The complete data set was binned into ten selected time spans to test whether the main period evolves over time. The reason that the data were binned into selected time intervals was to avoid uncertainties arising from the limitations of unevenly spaced data. The next section describes how the uncertainties in the periods were estimated. The averaged Julian date for each selected portion of the data, as well as the peak period with its power and associated uncertainty as described below, are given in Table 2.1. Figure 2.10 demonstrates how the period of BC Cyg decreased from 700 to 688 days over the interval spanned by the observations.

A noticeable feature of the time-averaged  $\langle B \rangle$  estimates for BC Cyg is that the star's brightness

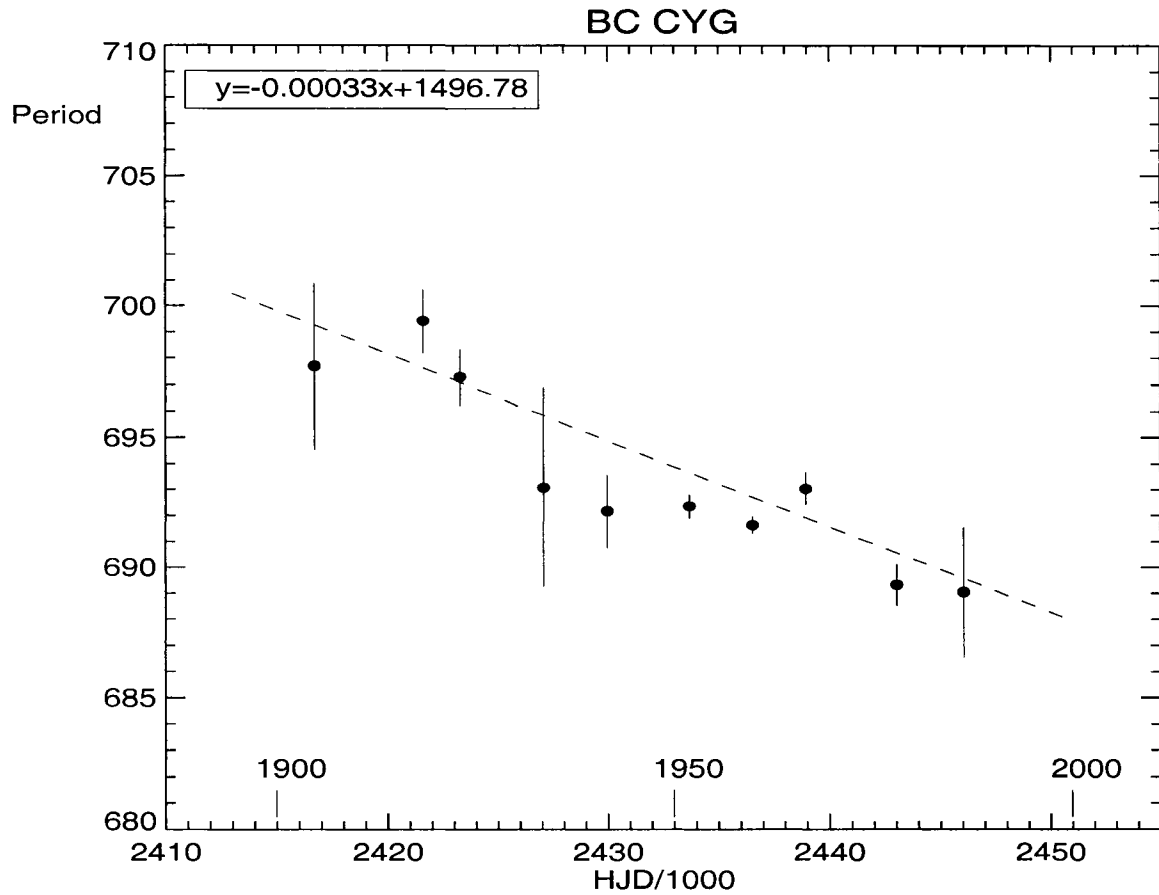


Figure 2.10: The period of BC Cyg decreased from 700 to 688 days over the interval spanned by the observations. A least squares fit was made to the data, which is illustrated along with the estimated uncertainties.

appears to evolve with time, as indicated by the data of Figure 2.11, where we show the entire data set averaged by running means over 50-day intervals. Such a systematic temporal change might be tied to the star's main cyclical variations, which is why it was considered essential to test for such an effect.

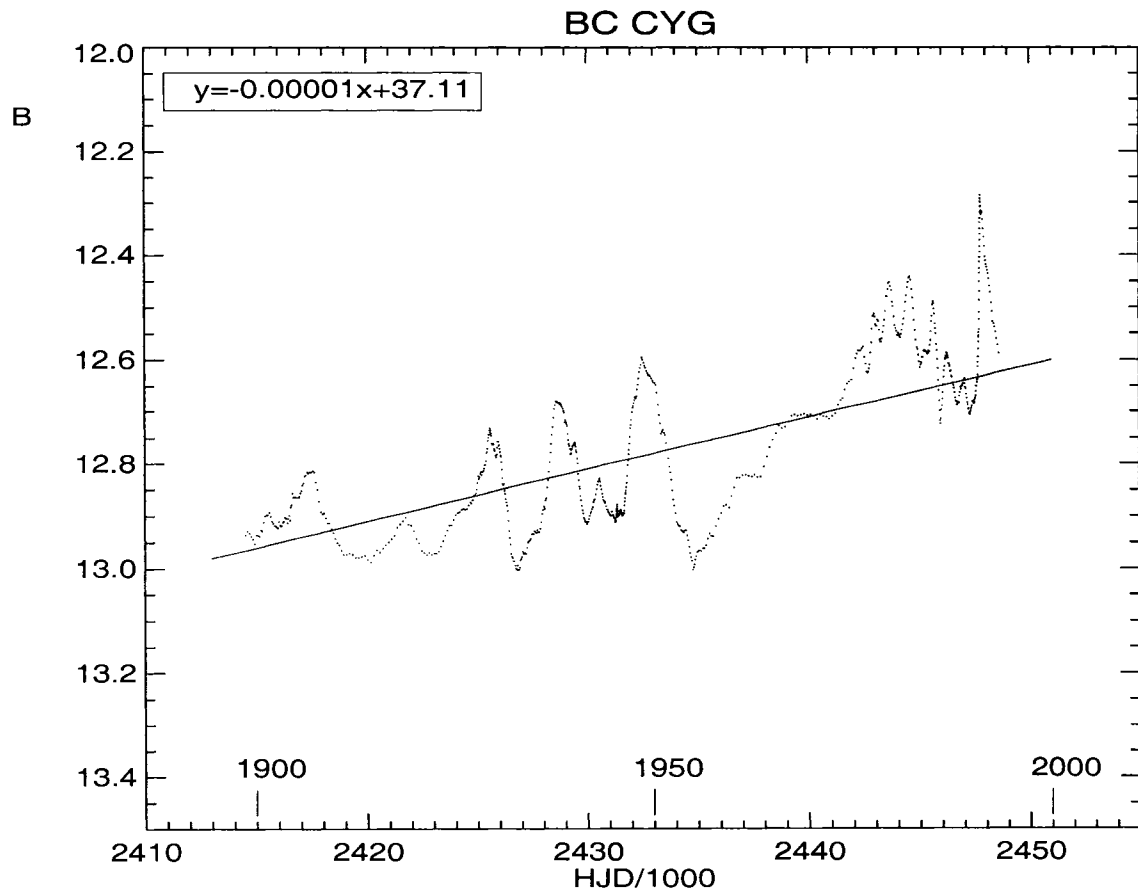


Figure 2.11: The evolution of the average brightness of BC Cyg as derived from running 50-day means of the original data sample. A trend line was fitted to the data by means of a least squares analysis.

## 2.6 Uncertainties In Period Determinations

As noted by Fernie (1989), the problem of finding the actual points of inflection (maxima, minima) in variable star light curves, along with their associated uncertainties, from noisy data, received an elegant solution by Kwee and van Woerden (1956, hereafter KvW), based upon work originating with Hertzsprung (1928). The technique involves fitting a parabolic curve to the calculated uncertainties as a function of the dependent variable, and using the parameters of the fitted parabola to estimate the likely dispersion in the dependent variable. We have used the same method here to fit a parabola to the time series data near the peak period derived from the power spectrum analysis in order to estimate the uncertainties in the periods derived from restricted temporal sequences isolated from the full light curve data set.

KvW show that a parabola that fits the power spectrum peak can be described by the equation

$$Y = aX^2 + bX + c, \quad (2.7)$$

where  $Y$  represents power ( $P$ ), and  $X$  is time or frequency. For the co-efficients  $a$ ,  $b$ , and  $c$  of the fitted parabola, the uncertainty in the period is given by the standard error of the mean dispersion in time values,  $\sigma$ , where

$$\sigma^2 = (4ac - b^2)/4a^2(Z - 1), \quad (2.8)$$

where  $Z = N$ , the number of data points. Note that the appropriate data to use in the equation are the power values  $P$  as a function of time rather than frequency.

Actual power spectra can exhibit fluctuations near maximum caused by incompleteness of the data or by aliasing effects. To exclude alias signals, the time ranges around the period peak were chosen in a manner to isolate the main peaks in the power spectra, as in Figure 2.12. If there was fine structure in the period peak, only those (power, time) pairs that delineated the envelope of the peak were used. That provided a more accurate fitting procedure. In the *IDL* programming environment, the function POLY-FIT performs the necessary task. It was used to perform a non-linear fit to

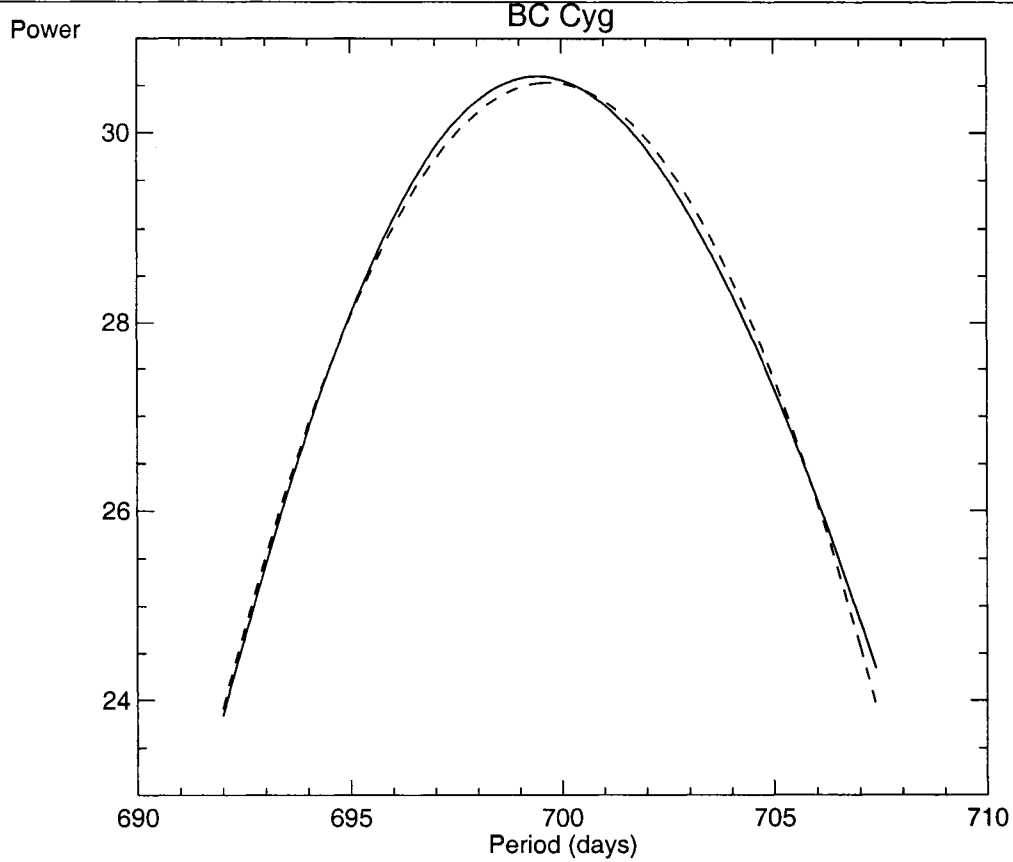


Figure 2.12: A sample power spectrum of the envelope around the period peak.

the narrow region about the highest peak in the total power spectrum calculated as a function of estimated period. A second-order, least squares, non-linear, fitting routine was used to match the main power spectrum peak with a parabola to determine its co-efficients, and a script was written in IDL to perform the fitting routine. The same procedure was repeated for each of the ten sub-samples selected from the entire data set. Table 2.1 is a summary of the data for the frequency, along with the highest power and period peak in each selection of light curve data obtained by using the TS software, along with the corresponding power and estimated uncertainty or sigma, the number of data points involved in the run, the mean Heliocentric Julian Date (HJD), and the time span for each interval used to obtain the sample.

Table 2.1: A summary of the data for the frequency with the highest power and period peak, the corresponding power and sigma, number of data points used in the fit,  $\langle \text{HJD} \rangle$ , and the duration of each interval in the sample.

Frequency	Period (days)	Power	$\sigma$ (days)	N	$\langle \text{HJD} \rangle$	Time span (HJD)
0.0014332	697.71	4.31	$\pm 3.19$	123	2416706	2411584-2421840
0.0014297	699.43	30.59	$\pm 1.23$	264	2421620	2411584-2427641
0.0014341	697.29	46.34	$\pm 1.05$	337	2423288	2411584-2430258
0.0014428	693.07	49.72	$\pm 3.83$	211	2427072	2423637-2430092
0.0014447	692.18	58.27	$\pm 1.41$	434	2429979	2423637-2438466
0.0014443	692.36	87.75	$\pm 0.45$	866	2433694	2423637-2450284
0.0014458	691.65	88.59	$\pm 0.32$	742	2436533	2411584-2450284
0.0014429	693.04	69.60	$\pm 0.62$	605	2438946	2428021-2450284
0.0014506	689.33	64.34	$\pm 0.80$	407	2443024	2432030-2450284
0.0014512	689.06	58.30	$\pm 2.52$	296	2446047	2441899-2450284

---

## 2.7 Period Estimates for a Few Other SRC Variables

Shown here are light curves and power spectra for a few other SRC variables, AD Per, RS Per, S Per, SU Per and YZ Per, Alpha Her, T Cet, as well as power spectra for the SRC variables AH Sco, VX Sgr and W Tri mentioned in section 2.2. Table 2.2 is a summary of the results for the main period estimates. The last line of the table lists the periods given in the GCVS. Note that the larger time spans of observation in the AAVSO database generate quite different periods of variability for these SRC variables than the values given in the GCVS, which were invariably based upon data obtained over much shorter time spans. Clearly it is advantageous for the study of such stars to have very long time spans of observation available.

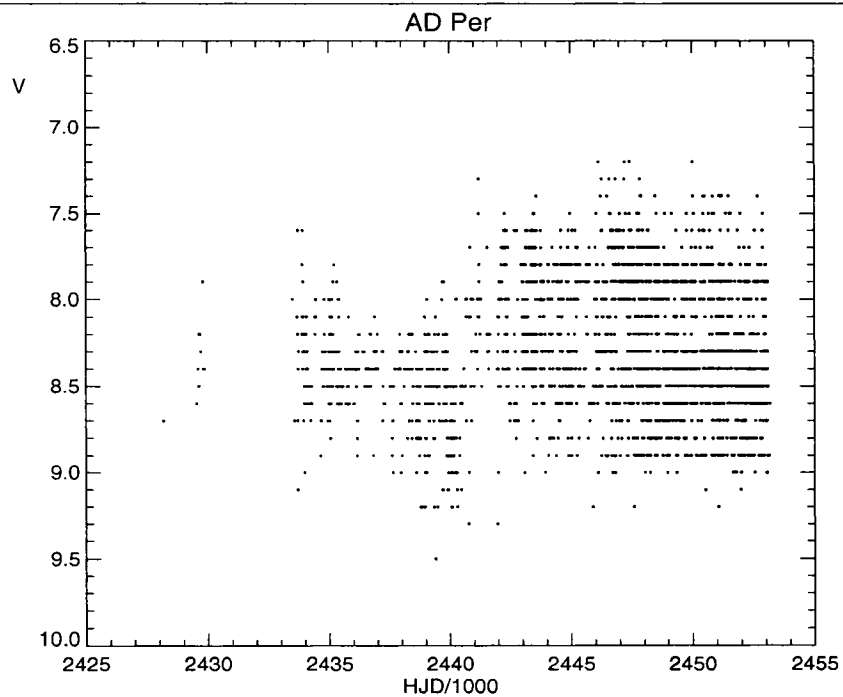


Figure 2.13: The light curve of the SRC variable AD Per in the V band, data courtesy of the AAVSO international database (Henden 2006).

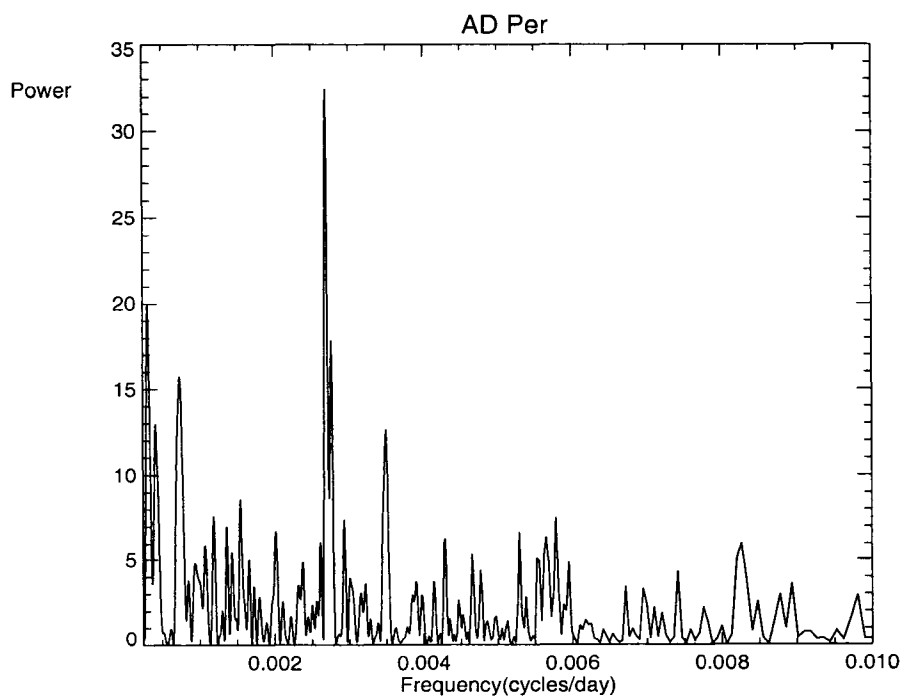


Figure 2.14: The power spectrum of AD Per.

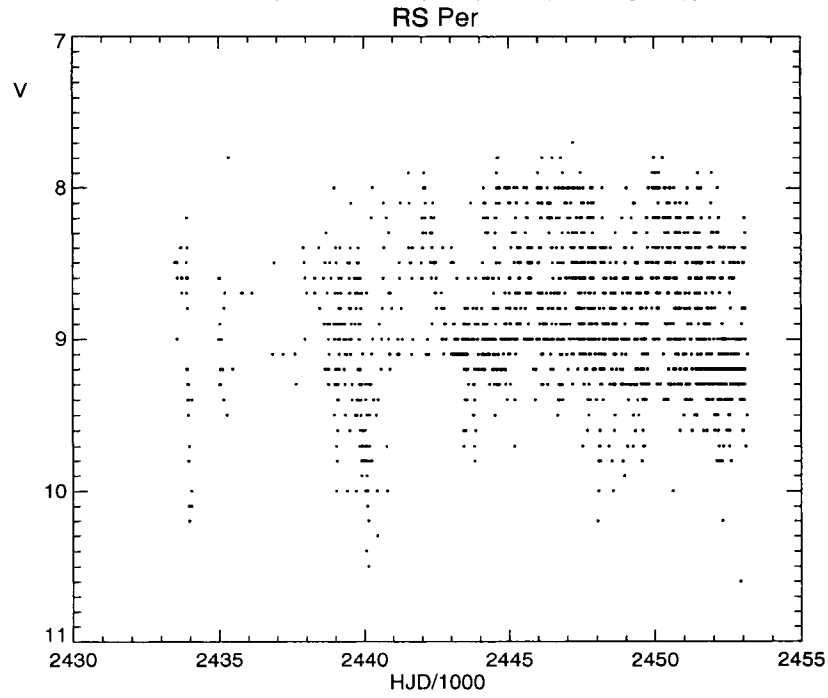


Figure 2.15: The light curve of the SRC variable RS Per in the  $V$  band, data courtesy of the AAVSO international database (Henden 2006).

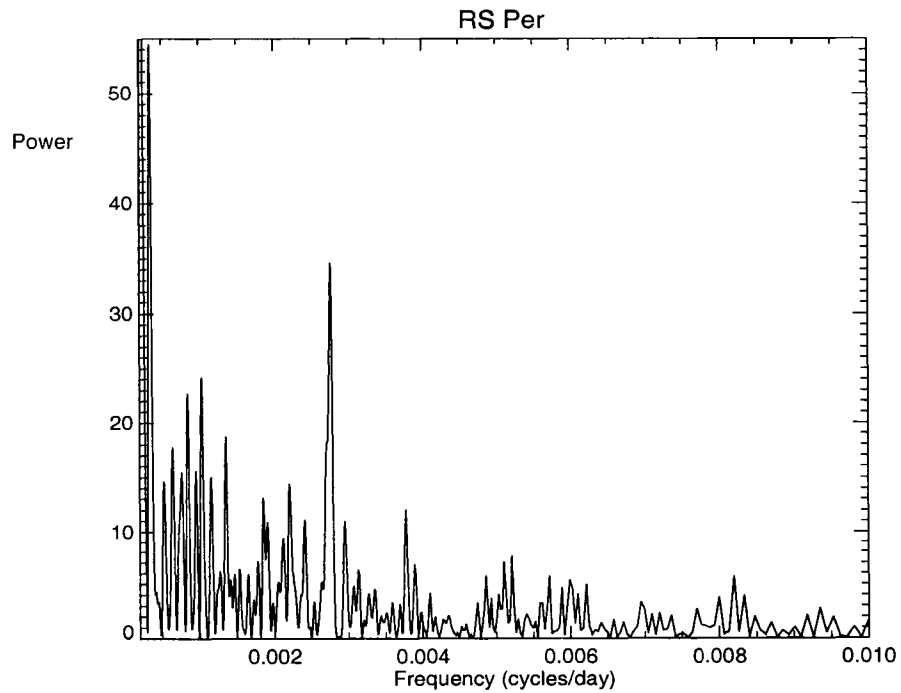


Figure 2.16: The power spectrum of RS Per.

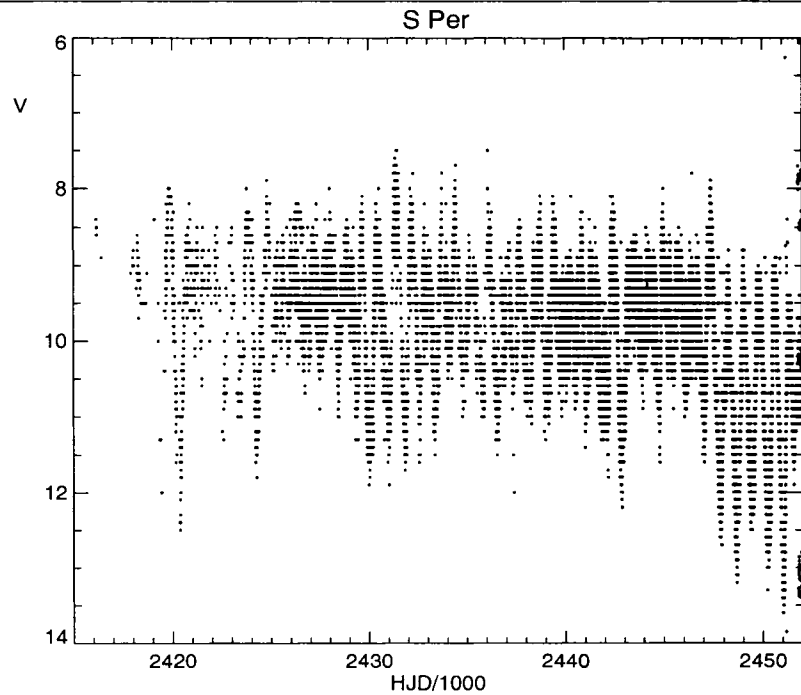


Figure 2.17: The light curve of the SRC variable S Per in the *V* band, data courtesy of the AAVSO international database (Henden 2006).

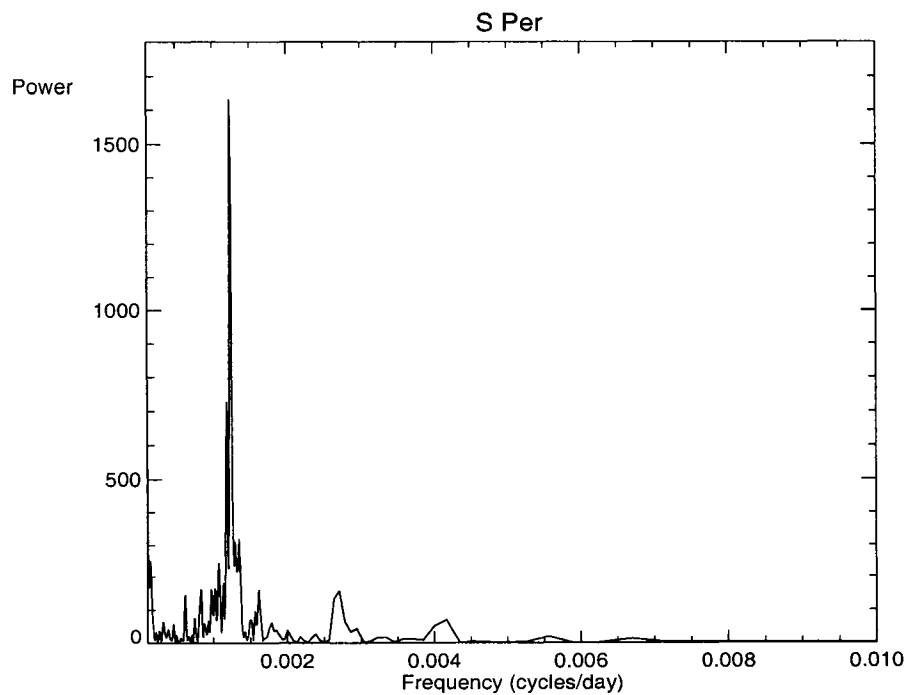


Figure 2.18: The power spectrum of S Per.

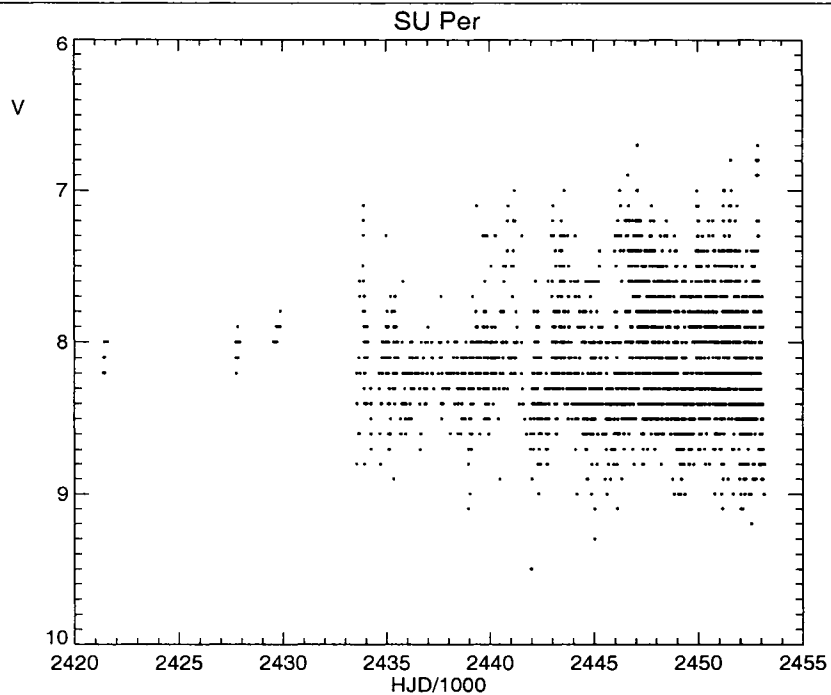


Figure 2.19: The light curve of the SRC variable SU Per in the V band, data courtesy of the AAVSO international database (Henden 2006).

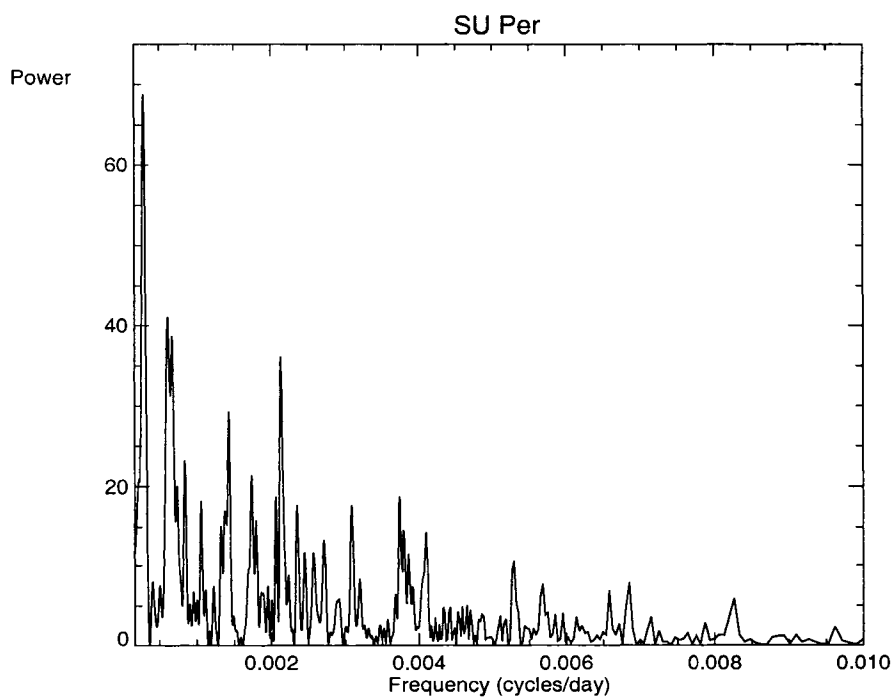


Figure 2.20: The power spectrum of SU Per.

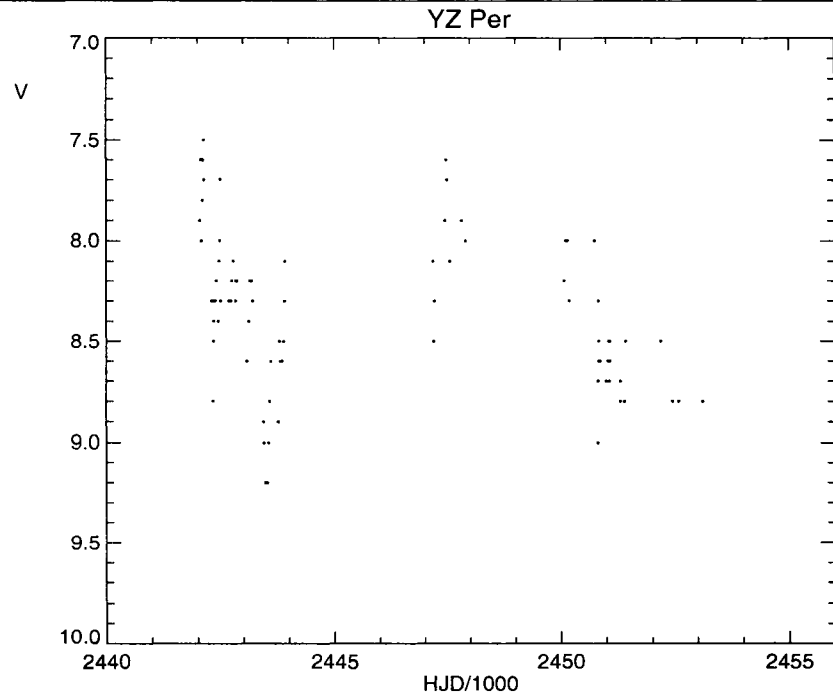


Figure 2.21: The light curve of the SRC variable YZ Per in the  $V$  band, data courtesy of the AAVSO international database (Henden 2006).

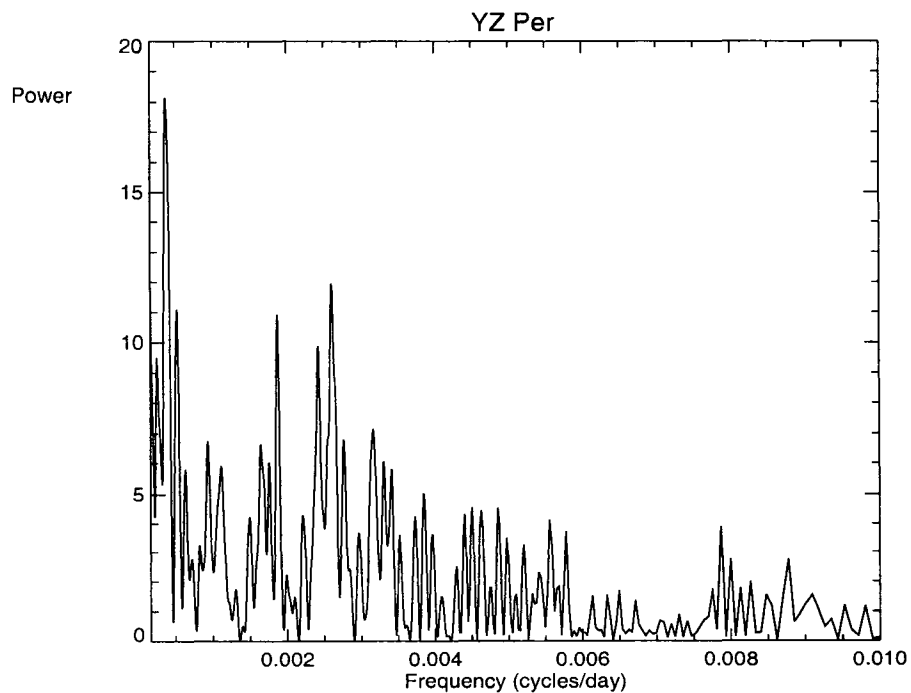


Figure 2.22: The power spectrum of YZ Per.

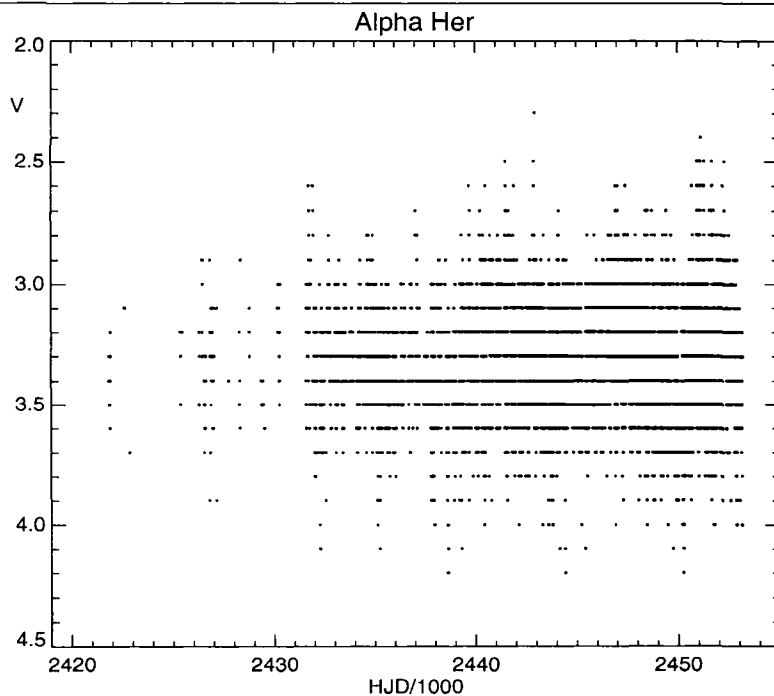


Figure 2.23: The light curve of the SRC variable Alpha Her in the  $V$  band, data courtesy of the AAVSO international database (Henden 2006).

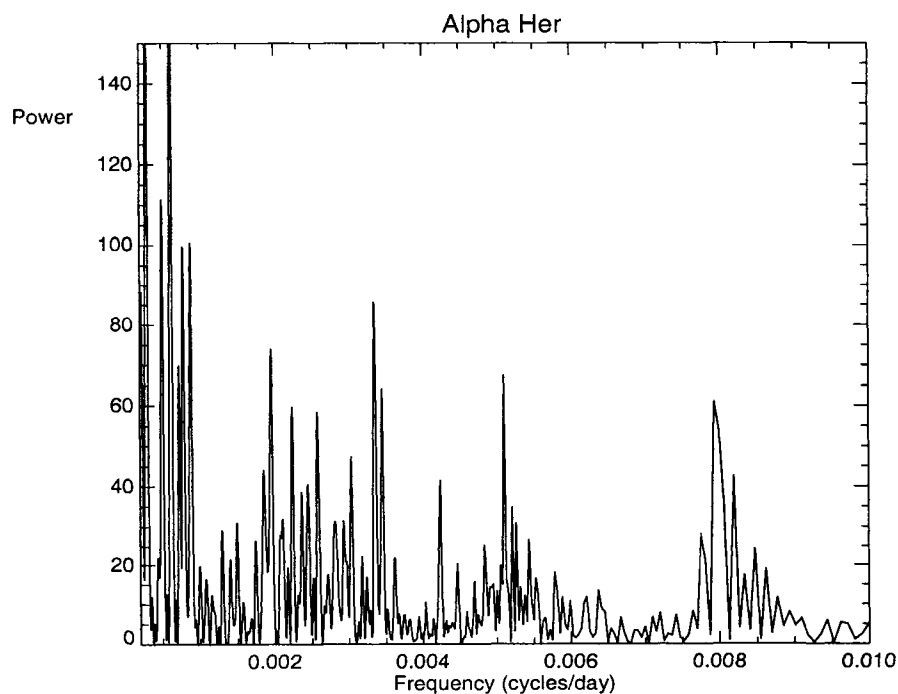


Figure 2.24: The power spectrum of Alpha Her.

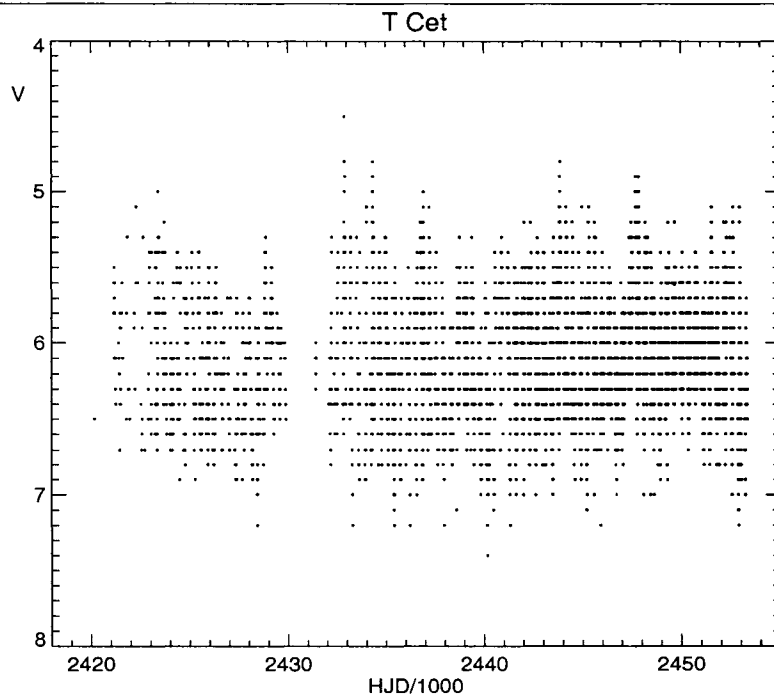


Figure 2.25: The light curve of the SRC variable T Cet in the  $V$  band, data courtesy of the AAVSO international database (Henden 2006).

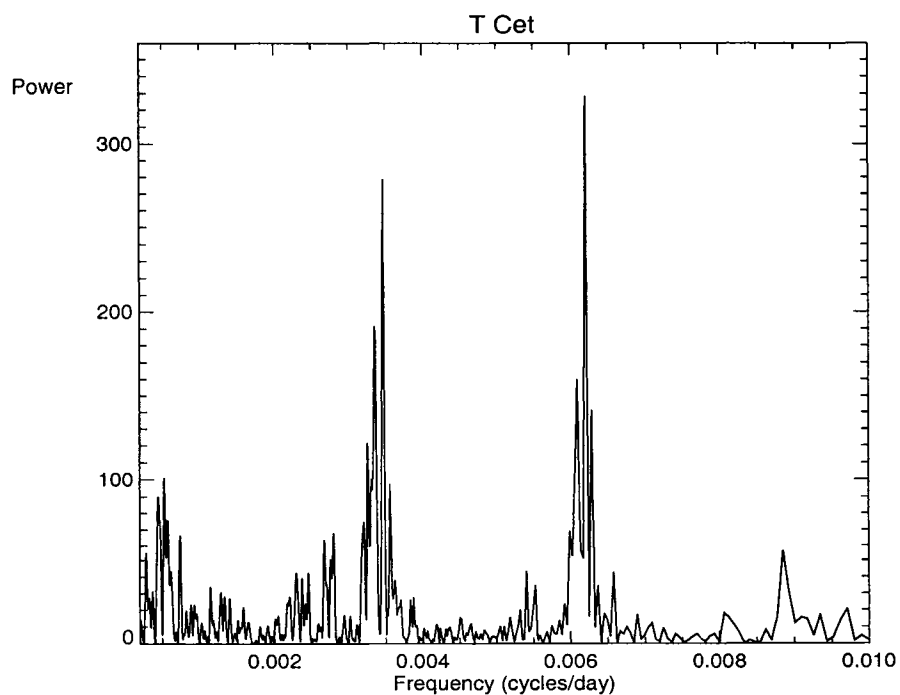


Figure 2.26: The power spectrum of T Cet.

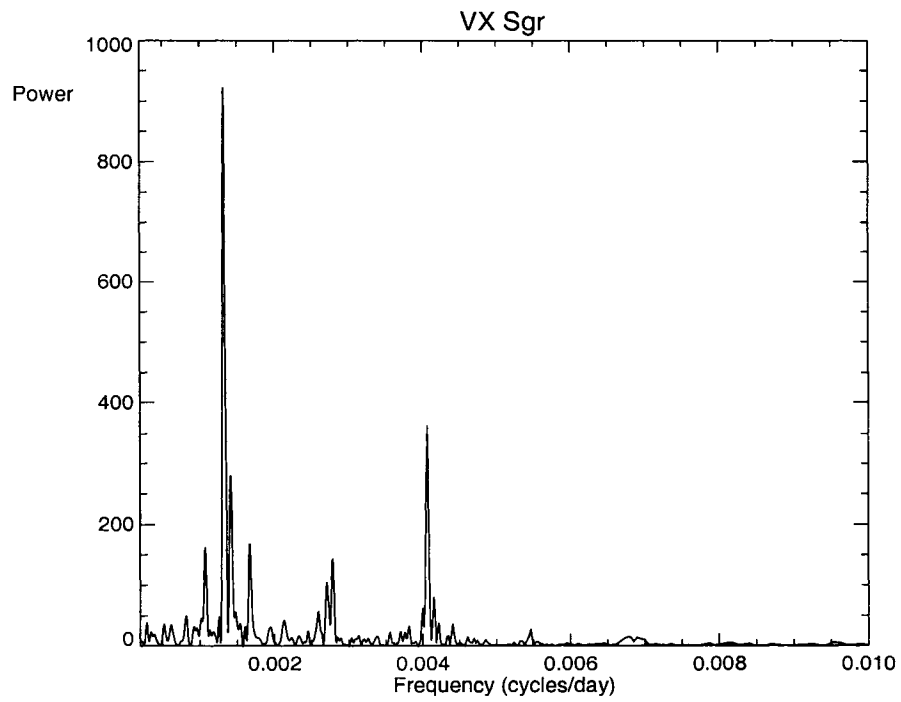


Figure 2.27: The power spectrum of VX Sgr.

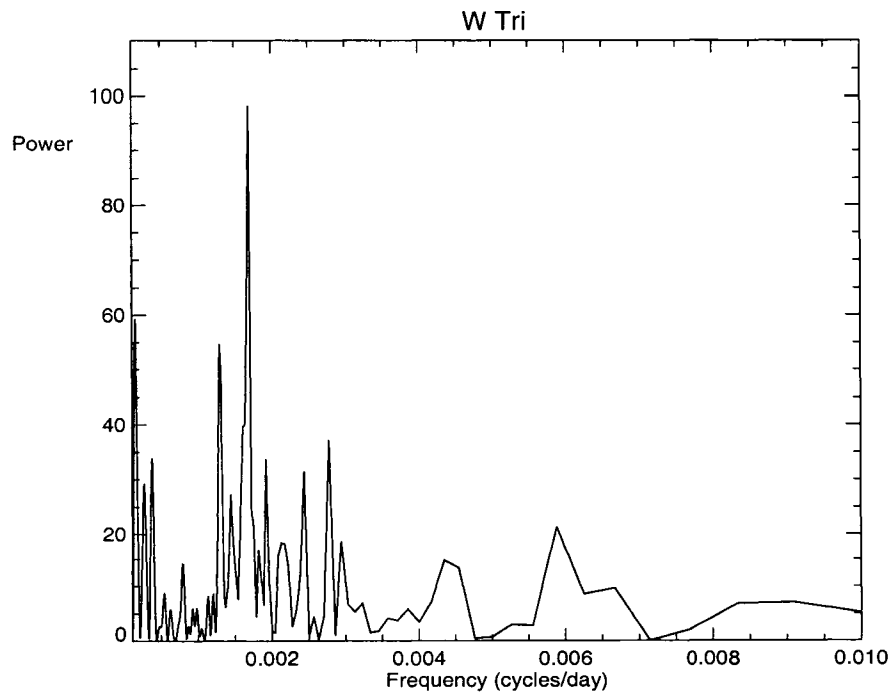


Figure 2.28: The power spectrum of W Tri.

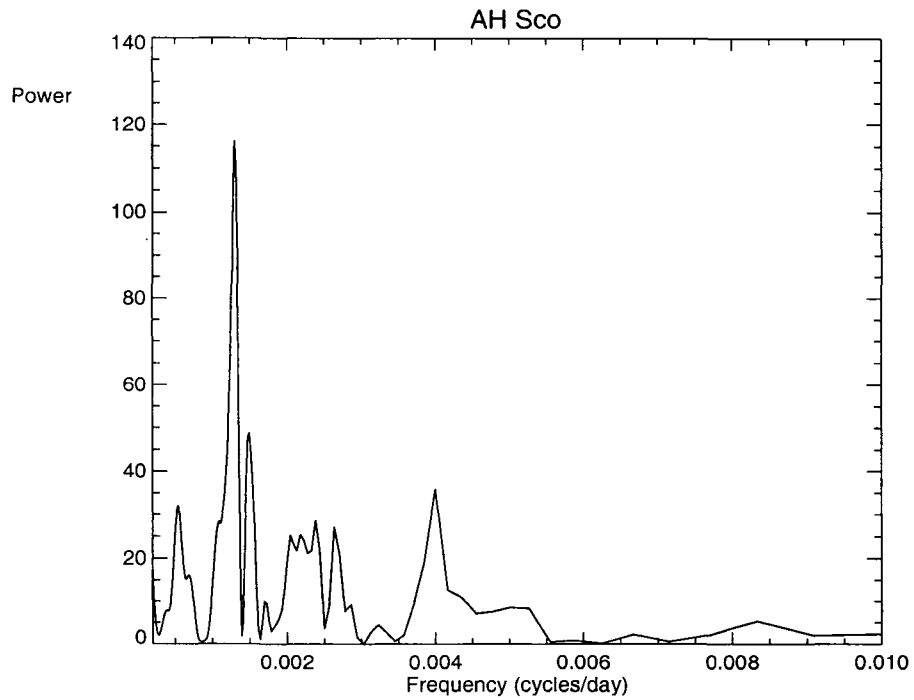


Figure 2.29: The power spectrum of AH Sco.

Table 2.2: A summary of the peak period for the above SRC variables.

Star	Period (days)	$\sigma$ (days)	GCVS P (days)
AD Per	371	0.1	362.5
RS Per	362	0.1	244.5
S Per	807	0.2	822
SU Per	469	0.4	533
YZ Per	384	0.4	378
$\alpha$ Her	116	0.4	?
T Cet	288	0.5	158.9
VX Sgr	757	0.2	732
W Tri	592	0.1	108
AH Sco	769	0.9	713.6

## 2.8 Non-linear Least Squares Fitting

A non-linear least squares fit was used to determine other parameters associated with BC Cyg after Fourier analysis was used to provide reliable estimates for the main periodicity. The quantities half-amplitude  $A$ , phase  $\phi$ , and an average magnitude scaling factor (zero point)  $\bar{m}$ , are needed to completely describe a sine function corresponding to each frequency  $\nu$ :

$$y(i) = A \sin(2\pi\nu x(i) + \phi) + \bar{m}, \quad (2.9)$$

where  $x(i)$  is the time of sampling each data point, and  $i = 1, \dots, N$  data points. The fit was made using the routine LM-FIT, a library program in IDL. LM-FIT requires that the user make reasonably accurate (to within a few percent) initial guesses for the frequency, phase, average magnitude, and amplitude. The fit was performed multiple times, each time selecting the initial parameters at random from a range of expected values from which the best fitting sine function was established. In order to increase the probability of finding the lowest possible  $\chi^2$  value for the converged fit, the number of iterations was adopted to be 3000 for each initial guess of a fitted sine function.

For a given set of data points, the frequency with the highest power was chosen from a plotted power spectrum. The routine LM-FIT was then used to perform a non-linear, single-sine, least squares fit to the data, using the dominant frequency and guesses for  $A$ ,  $\phi$ , and  $\bar{m}$ . The best (lowest  $\chi^2$ ) converged fit was then subtracted from the data, that is, the data were “prewhitened”. A new power spectrum was then created for the prewhitened data to see if any secondary period was apparent in the absence of the dominant period. If any further periodicities were present, their functional dependence was individually fitted to the data using a single-sine function with LM-FIT. The procedure was repeated until no further periodicity of reliable amplitude or power was detectable.

## Chapter 3

# The Period Searches and Their Results

As was shown in Figures 2.9, the original power spectrum of BC Cyg contains a number of peaks with lower power relative to the highest peak, which created the motivation for searching for any other possible periodicities. To search for other periods, part of the light curve with the most evenly sampled data points, spanning from HJD 2442000 to 2449000 (Figure 3.1), was chosen in order to get a converged solution using LM-FIT. Because the rest of the dataset was not well enough sampled, no converged solution could be found using LM-FIT.

The first step in the reduction was to use the non-linear least squares routine LM-FIT to determine accurate parameters for the primary frequency. A power-spectrum plotted by TS for the selected part of the dataset was used to obtain the range of initial guesses for the amplitude ( $A_1$ ) and period ( $P_1$ ). The initial range of values for  $\bar{m}$ , the mean magnitude of the data, could be estimated reasonably by examination of the light curve. As  $\phi$  was completely unknown, it was allowed to be chosen at random between 0 and  $2\pi$ .

After 3000 iterations, the program converged on the following best-fitting parameters with the given standard deviations (sigma):

$$A_1 = 0.57 \pm 0.12, P_1 = 686 \pm 23.47, \Phi_1 = 3.17 \pm 5.2, \text{ and } \bar{m} = 12.62 \pm 0.02$$

with a reduced  $\chi^2$  value of 0.1.

Figures 3.2 and 3.3 show power-spectra resulting from the originally selected dataset before and after prewhitening by the above estimated parameters for the primary periodicity. After the main periodicity has been removed from the BC Cyg data, we do not expect to see any peaks of importance in comparison to the original power spectrum, which turns out to be the case. None of the remaining peaks is significant relative to the measuring uncertainties of  $\pm 0^m.1$  to  $\pm 0^m.2$  in the eye estimates of  $B$ , as shown in Figure 3.4. Figure 3.5 also shows the residual light curve after removal of a sine wave with the above estimated parameters. Figure 3.6 shows the fitted sine function using the main frequency on the original light curve.

---

The remaining scatter about the best-fitting sine wave can be readily accounted for by uncertainties in the original observations as well as by possible variations in light amplitude from one cycle to the next, a common feature of most semi-regular variables. BC Cyg is no different from other stars of its class in that regard.

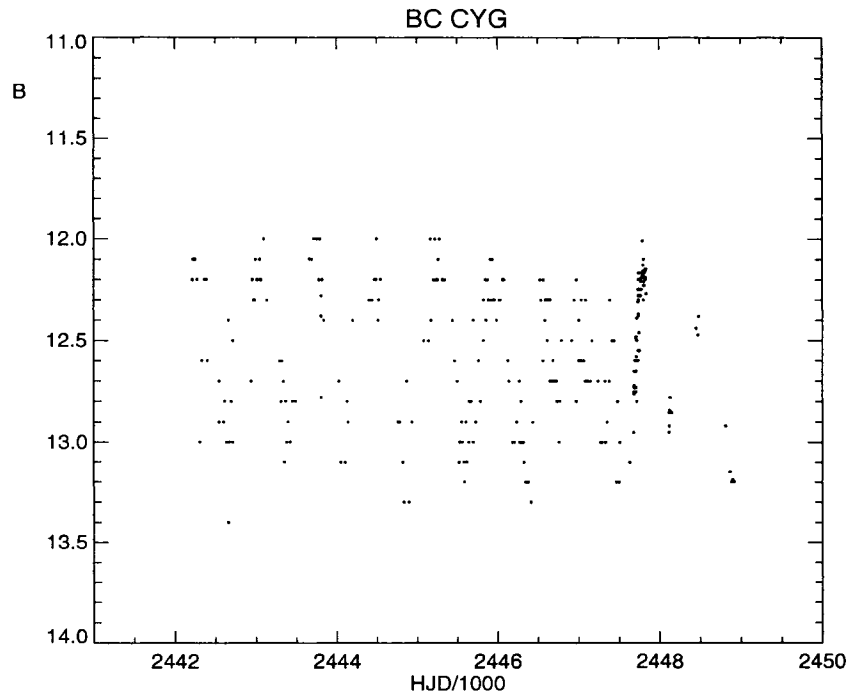


Figure 3.1: The selected part of the light curve of BC Cyg.

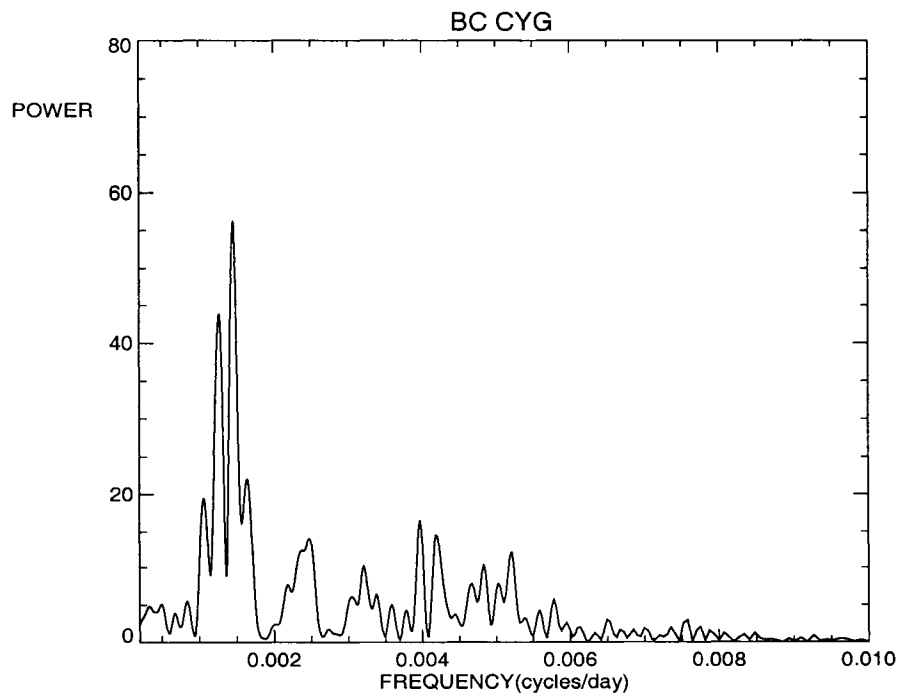


Figure 3.2: Power spectrum of the original data spanning from HJD 2442000 to 2449000.

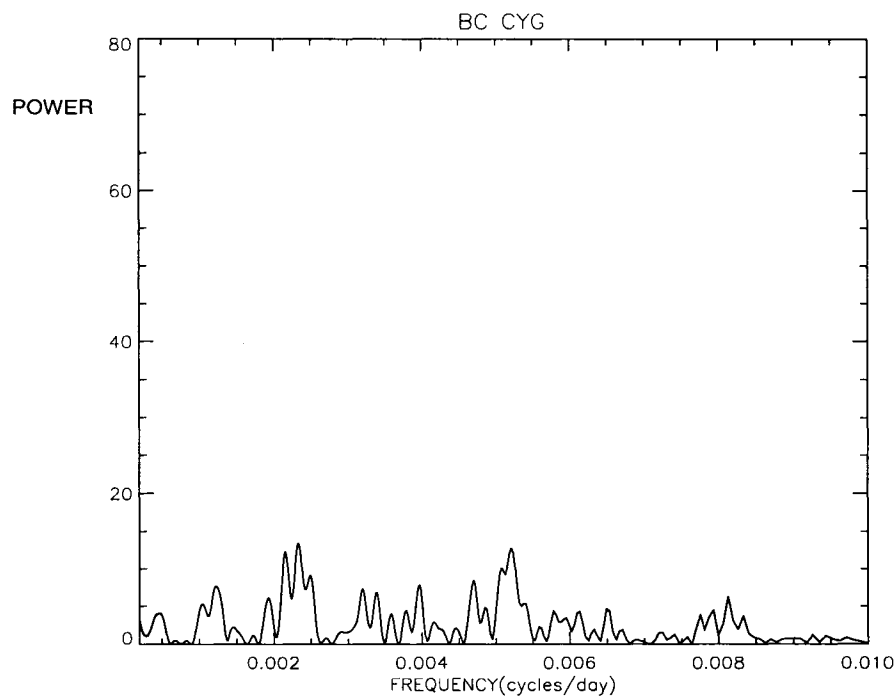


Figure 3.3: Power spectrum of the original data after prewhitening with a fitted sine function of the form:  $B = A_1 \sin((2.0\pi h j d / P_1) + \Phi_1) + \bar{m}$ .

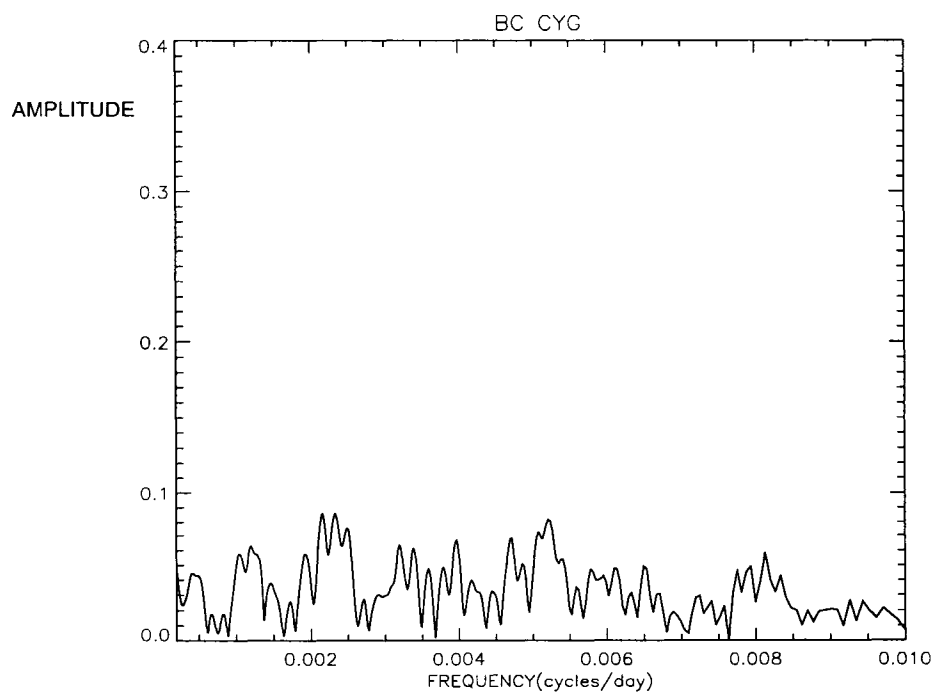


Figure 3.4: A plot of Fourier amplitude versus frequency of the residual data (original -  $P_1$ )

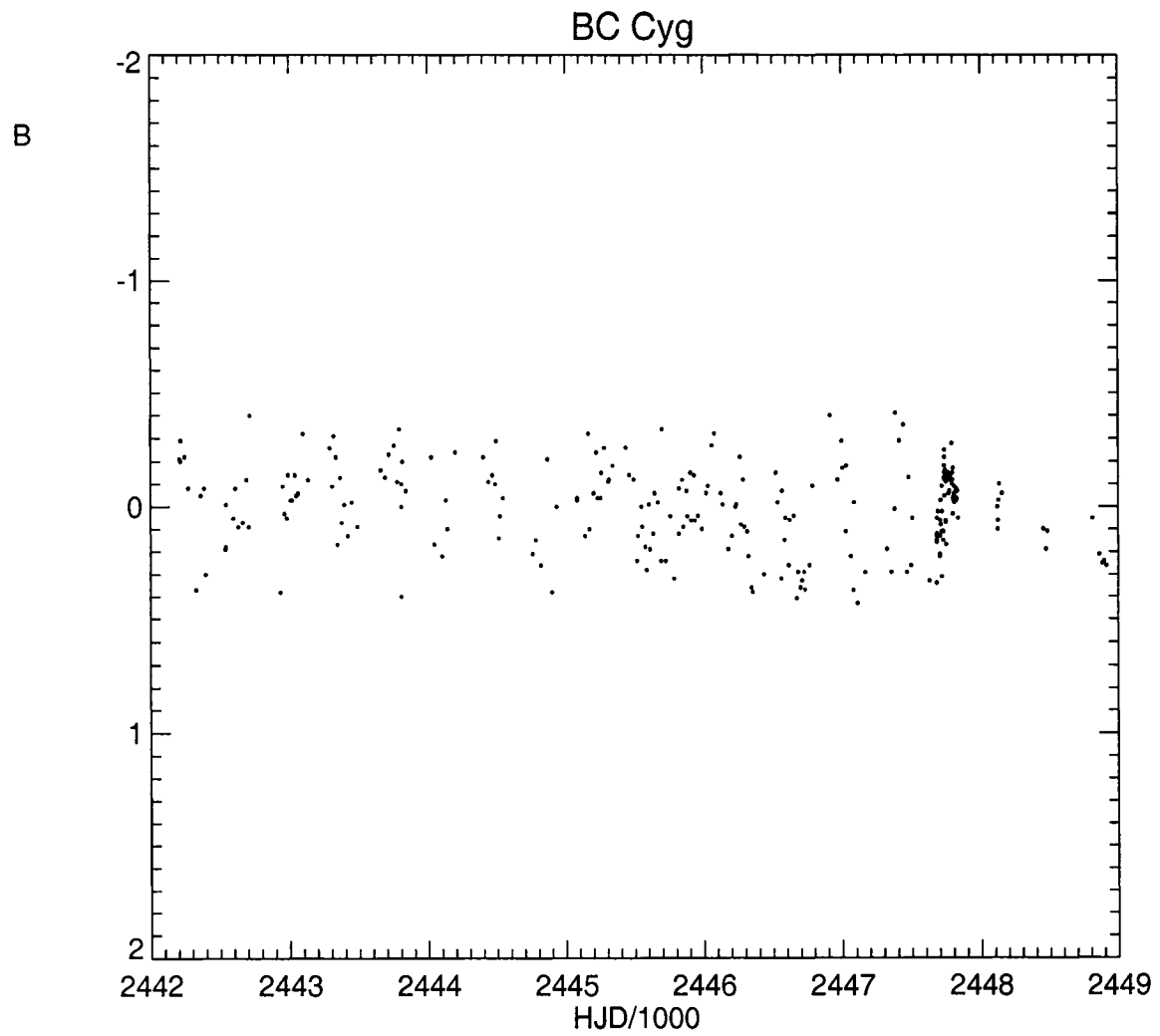


Figure 3.5: Residuals in the light curve of BC Cyg after fitting the data using a single period  $P_1$

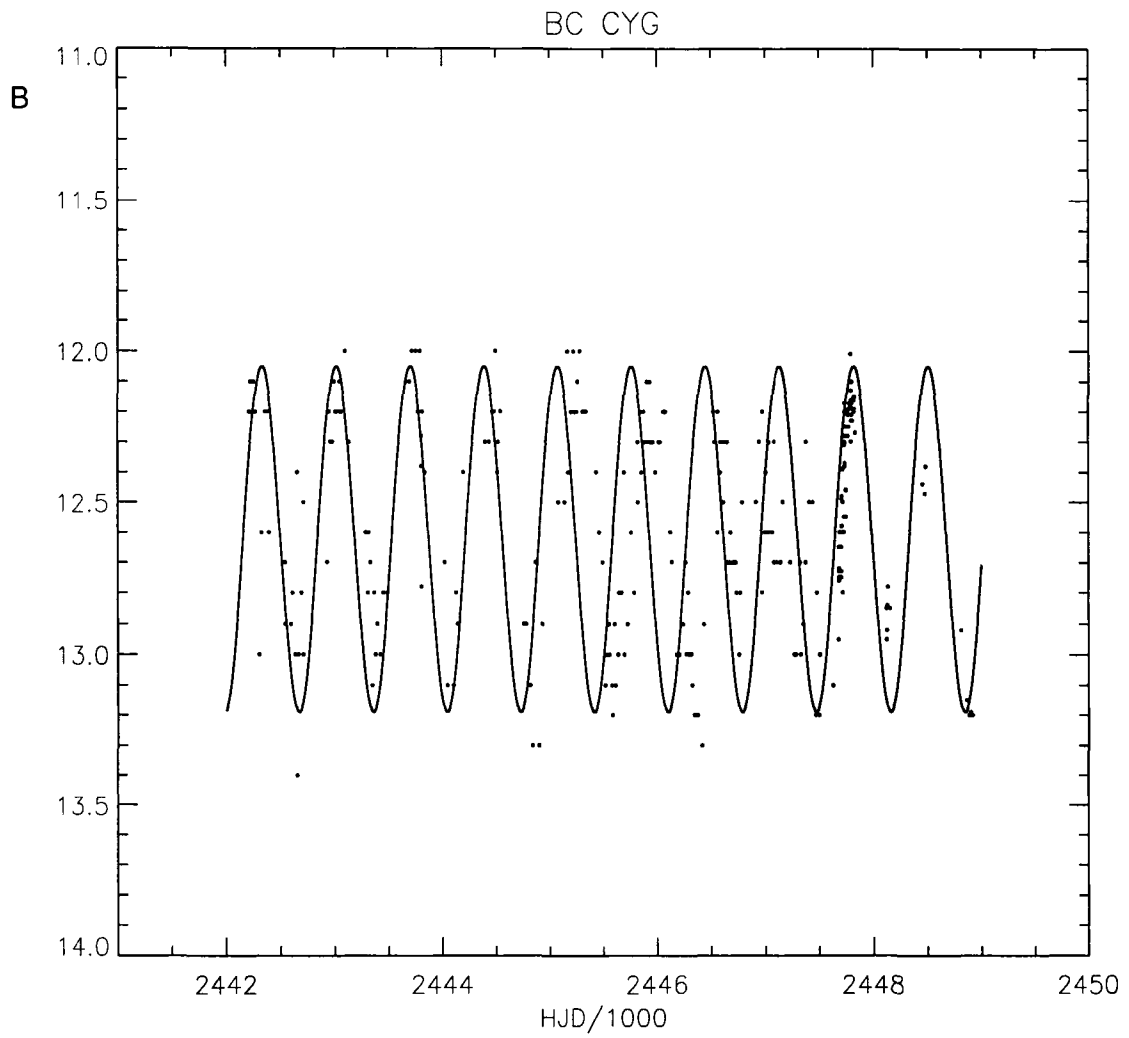


Figure 3.6: Light curve of BC Cyg with the main frequency fitted on it.

# Chapter 4

## Implication of the Results

### 4.1 Brightness Variation

The observed 700-day brightness variations in BC Cyg must be attributed to radial pulsation. That was demonstrated by Stothers (1969b) 37 years ago using adiabatic models. We performed a simple test of those original results using software from R. G. Deupree (private communication) that generated simple non-adiabatic models for given input parameters of mass, radius, and surface temperature, and then performed a pulsation test with the resulting model. For the parameters of BC Cyg derived below, the test generated pulsation periods that were similar in magnitude to the observed 700-day periodicity of BC Cyg. More detailed models by Li and Gong (1994) produce comparable results.

Because BC Cyg is a member of a well studied open cluster, Berkeley 87, its reddening and distance can be obtained directly from other cluster stars. According to Table II in Turner and Forbes (1982), space reddenings of  $E_{(B-V)}(B0) = 1.554, 1.553, \text{ and } 1.545$ , colour excesses adjusted to equivalent values for B0 stars observed through the same amount of interstellar extinction, are estimated for stars numbered 53, 58, and 85, which are close enough to BC Cyg (star 78) to be considered as reference stars for its reddening (Figure 4.1). The average value,  $\bar{E}_{(B-V)}(B0) = 1.551 \pm 0.003$ , is a good estimate for the space reddening of BC Cyg. Figure 4.1 is the finding chart for Berkeley 87, the large circle representing the outer cluster boundary determined from star counts (diameter = 16 arc min), and the cross depicting the location of the cluster center (Turner and Forbes 1982).

Blue magnitudes in the Johnson system are affected by the colour of a star, so colour excess is highly dependent on the temperature of a star (e.g., Fernie 1963). A reddening of  $E_{(B-V)}(B0) = 1.55$  corresponds to  $E_{(B-V)} = 1.32$  for a star with the colour of a M3.5 Ia supergiant. Since such stars have  $(B - V)_0 = 1.75$  (Lee 1970), an observed value of  $(B - V)_{obs} = 3.07$  is expected for BC Cyg, given its spectral type of M3.5 Ia.

---

Turner and Forbes (1982) obtained a distance modulus of  $V_0 - M_V = 9.88$  and a distance of  $d = 946 \pm 26 pc$  to Berkeley 87. But ZAMS (zero-age main sequence) stars in the cluster CMD (colour-magnitude diagram) appear to be more consistent with a slightly larger distance, up to  $V_0 - M_V = 10.25$ , or a distance of  $d = 1120 pc$ .

$M_V$  and  $M_{bol}$  for BC Cyg depend upon the average value (zero point) for its  $V$  magnitude. The extremes are given in Table 6.1 in the Appendix. Bolometric corrections are very uncertain for M supergiants, which have very low temperatures by astrophysical standards. Although there are a few sources of bolometric corrections for cool stars, the specific bolometric correction applying to an individual star is very sensitive to its inferred temperature. Given existing uncertainties in the effective temperatures of cool M supergiants, the BC scale for such stars remains very uncertain (e.g., Johnson 1963; Flower 1977).

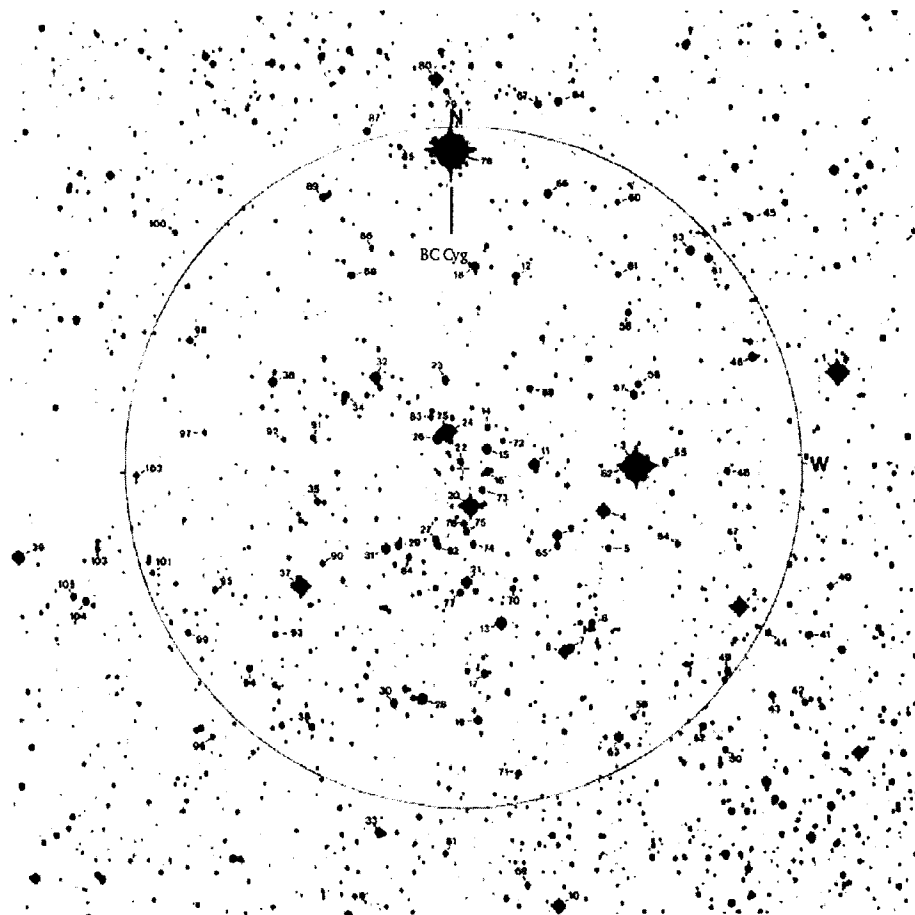


Figure 4.1: A finding chart for Berkeley 87, as derived from the POSS E-plate of the region. North is toward the top of the image, and east is toward the left hand side of the image.

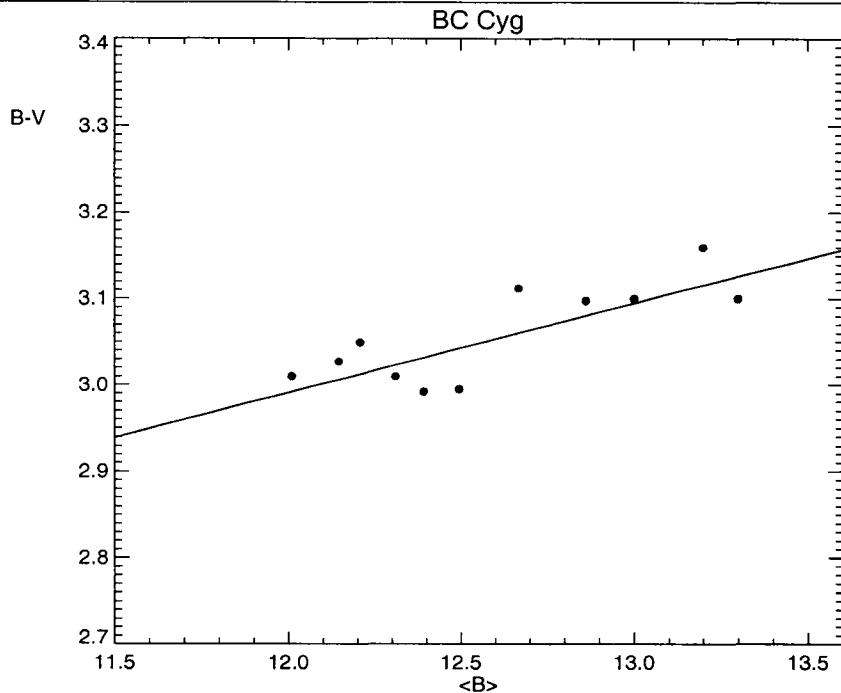


Figure 4.2: The observed colours of BC Cyg as a function of the stars's photographic magnitude as derived from averages of AAVSO visual estimates combined with photographic estimates of the star made within roughly ten days of each other.

From AAVSO eye estimates of the visual magnitude of BC Cyg in combination with its photographic ( $B$ ) magnitude estimated from survey plates, it is possible to track changes in the colour of the star as it brightens and fades, as illustrated in Figure 4.2. The input data for Figure 4.2 actually consist of 66 data points selected from observations closely coincident in time, while the plotted points represent running averages of the data closely adjacent in  $B$  magnitude. The data appear to define a trend line when averaged in such fashion. It appears that the star gets redder (cooler, larger  $\langle B \rangle - \langle V \rangle$ ) as it gets fainter, bluer (hotter, smaller  $\langle B \rangle - \langle V \rangle$ ) as it brightens.

The original data exhibit sizable scatter and, in some cases, systematic errors presumably tied to the colour sensitivities of some AAVSO observers. Although the colour differences between maximum brightness and minimum brightness for BC Cyg are relatively small, amounting to ( $\sim 0.15$  in  $\langle B \rangle - \langle V \rangle$ ), they correspond to very large differences in bolometric correction, BC, of  $> 2^m$  (Lee 1970). Thus, while the photographic magnitude of BC Cyg increased by  $\sim 0.5$  magnitude over the past century, the star's bolometric luminosity apparently decreased by about the same amount over that interval, if the observed  $\langle B \rangle - \langle V \rangle$  colour decrease is accurate. If the associated

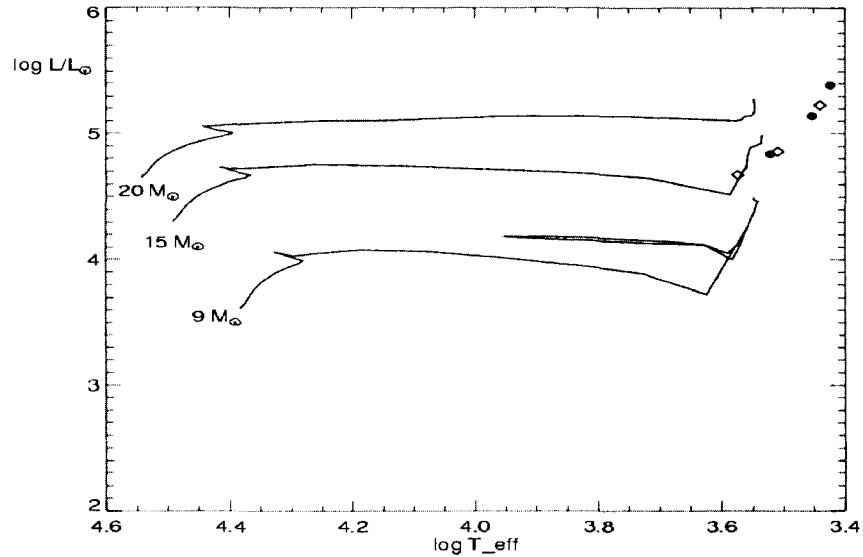


Figure 4.3: A theoretical H-R diagram showing evolutionary tracks for stars of  $9M_{\odot}$ ,  $15M_{\odot}$ , and  $20M_{\odot}$  and  $Z = 0.02$  (Schaller et al. 1992), and the estimated parameters for BC Cyg over its pulsation cycle around 1900 (filled circles) and 2000 (open diamonds).

colour changes and assigned bolometric corrections are correct, the star is most luminous when it is faintest visually and photographically. Such features require more investigation and independent confirmation.

It is instructive to show the corresponding position of BC Cyg in an H-R diagram. For that purpose, it is necessary to estimate its luminosity and effective temperature. The conversion of  $B$  and  $V$  magnitudes and colours into  $T_{\text{eff}}$  and  $\log(L/L_{\odot})$  depends directly on the effective temperatures and bolometric corrections adopted for M supergiants. The present calculations rely upon the parameters tabulated by Lee (1970), and may not be ideal. But an alternate source of such parameters for cool stars is not readily available.

In the H-R diagram of Figure 4.3, solid curves represent theoretical stellar evolutionary tracks for stars with original masses of  $9M_{\odot}$ ,  $15M_{\odot}$ , and  $20M_{\odot}$  and  $Z = 0.02$  (Schaller et al. 1992). The parameters for BC Cygni in 1900 at light maximum, light minimum, and mean light are shown by filled circles, those for 2000 by open diamonds.

It seems that BC Cygni has evolved downwards along the red supergiant branch towards lower

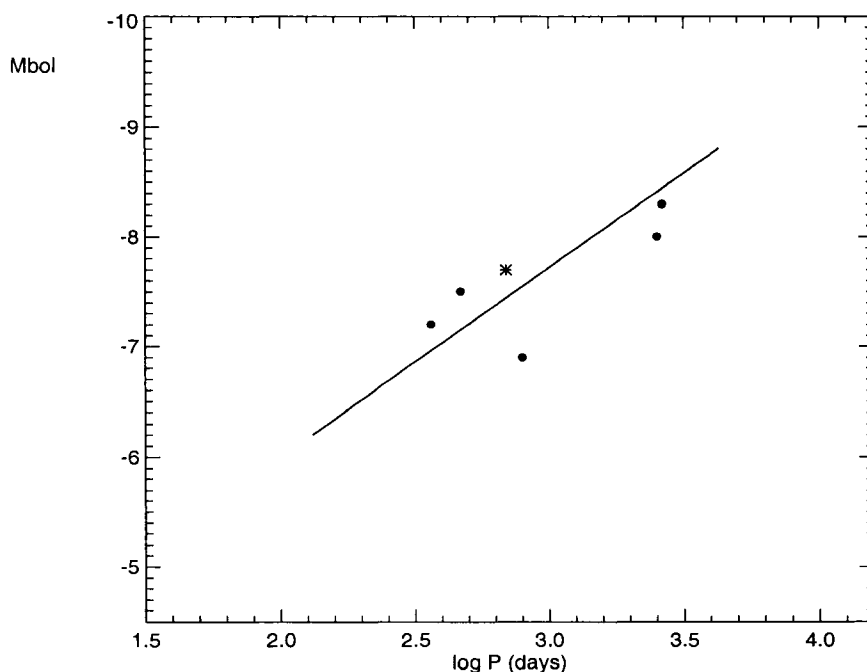


Figure 4.4: A period-luminosity relation for SRC variables in Per OB1 (filled circles) and BC Cyg (star) constructed from  $BV$  data for the stars. Shown for comparison is a theoretical pulsation model for Galactic red supergiants with  $Z = 0.02$  (solid line) from Guo and Li (2002).

luminosities over the past century, as confirmed by its slightly decreasing pulsation period (Figure 2.10) which must be related to a smaller mean radius. In order to construct the H-R diagram of Figure 4.3,  $Z = 0.02$  was chosen as the metallicity since most nearby Galactic variables of population I have heavy element abundances that are roughly solar (Guo and Li 2002).

It is certainly important to determine if the brightness change is intrinsic to the star, specifically, whether it is interior to the photosphere (for example, it might alternately be explained by the dispersal of an optically thin gas cloud around the star). The brightness change could also arise from some modification of the effective temperature that does not affect the radius, and that would not greatly affect the period. Existing stellar evolutionary models cannot replicate the observed changes in the star's parameters very well, according to the results of Figure 4.3. However, the time steps of the evolutionary models plotted in Figure 4.3 are in some cases less than half a century during the red supergiant stages, so stellar evolutionary changes in BC Cyg over the time interval studied here (a full century) are not unexpected.

The regular periodic nature of the star's brightness variations is clearly tied to pulsation, as

evident from the fact that BC Cyg, as well as SRC variables in Per OB1, follow a period-luminosity relation similar to that of Cepheids (Turner 2006). Figure 4.4 shows the calculated  $P$ - $L$  data for cluster M supergiant SRC variables (AD Per, RS Per, S Per, SU Per, YZ Per) in Per OB1 and Berkeley 87 (BC Cyg), for which both their  $M_{\text{bol}}$  and light curves were available.  $M_{\text{bol}}$  estimates for Per OB1 supergiants are adopted from data in Table 1 of Stothers (1969a), and periodicities for the stars were calculated using TS software with their visual light curves obtained from the AAVSO web site (Henden 2006). Also shown are predictions for the  $P$ - $L$  relation deduced from theoretical models which were constructed using a linear non-adiabatic pulsation analysis (Table 9) of Guo and Li (2002) for red supergiants with  $Z = 0.02$ .

## 4.2 Characteristics of the Light Curve

A single period,  $\sim 686$  days, was detected in BC Cyg over a restricted time interval using non-linear least squares fitting with a reduced  $\chi^2$  value of 0.1. The given reduced  $\chi^2$  is less than the expected value of unity for a perfect fit, which might arise from the unevenly spaced temporal sampling of the data. It is also possible that the star exhibits amplitude changes from cycle to cycle, a common feature of the late-type semi-regular variables.

Existing information on SRC variables is naturally incomplete because of the limited availability of observational data for them, and detection of periodicities is always accompanied by some uncertainties. Certainly an extensive analysis of the light curves of some of the other SRC variables listed in Chapter 2 displaying amplitude modulation might provide a clue regarding the source of the phenomenon, with results perhaps leading to a better understanding of the nature of brightness variations in such stars.

# Chapter 5

## Summary

The light curve of the M3.5 Ia supergiant BC Cygni, an important SRC variable, was examined in detail, particularly because its membership in the cluster Berkeley 87 provides basic information about its reddening, luminosity, mass, and evolutionary stage, parameters that are not always readily available for other members of the class. The recent collection of a century-long baseline of data on its brightness variations provides a wealth of material for analyzing the nature of the star's variability. As described here, an extensive period analysis was performed on the light curve of BC Cygni, and the evolution of the main periodicity was followed along with an estimate of its uncertainty calculated for 10 selected portions of the complete dataset. The period of BC Cyg decreased from 697 to 686 days over the interval spanned by the observations, while the time-averaged  $\langle B \rangle$  brightness of BC Cyg appears to have increased with time.

A single period of  $\sim 686$  days was found using non-linear least squares fitting with a smaller subset of the  $B$  data. A detailed study of the data for this data subset reveals no evidence for a second periodicity in the observations. The primary regular light variations in BC Cyg must therefore be tied to pulsation, although the long-term trend has another origin. The present study of BC Cygni is relatively unique, given that it is based upon data with a time coverage of over a century. That is a long enough interval that stellar evolutionary changes may be detected. Stellar evolutionary models for stars of roughly  $20 M_{\odot}$ , the likely mass of BC Cyg, exhibit noticeable changes on time scales as short as 35 years.

Estimates of pulsation periods were also derived for a few other SRC variables using data from the AAVSO database and power spectra generated by the TS software. The derived periods range from 116 to 822 days. The value of collected archival observations of brightness for members of the SRC class is demonstrated by the differences between the newly-derived pulsation periods for the variables with values cited in the GCVS. In some cases the original period estimates in the GCVS based upon data with limited temporal baselines are in error by as much as a factor of six. There have not been many period studies for SRC variables up until now owing to the lack of data with

---

lengthy temporal baselines. That illustrates the importance of such studies, given that pulsation period is a fundamental parameter for large and cool stars. Given the ease of detecting M supergiants over large Galactic and extragalactic distances, studies of the light variations in such stars continue to be of relatively high importance.

An optical calibration is presented for the period-luminosity relation of SRC variables, tied to M supergiants in the region of Per OB1 as well as BC Cyg in Berkeley 87. The results are compared with existing theoretical pulsation models for massive M supergiants based upon linear non-adiabatic pulsation analysis for stars pulsating in the fundamental mode. The theoretical P-L relation proves to be in very good agreement with the observational data for the calibrating M supergiants, and proves its usefulness for finding extragalactic distances. Since such stars are ultimately the source of Type II supernovae, detailed studies of their current behavior may prove useful as the stars come close to the ends of their evolutionary lifetimes.

## Chapter 6

# Appendix

### Tables of Data for BC Cyg

Table 6.1 contains estimated values of  $B$ ,  $V$ ,  $B-V$ ,  $(B-V)_0$  and  $M_V$  for BC Cyg at its faintest and brightest.

Table 6.2 is the blue band magnitudes from the collection of the Sternberg Observatory.

Table 6.3 is the blue band magnitudes from the collection of astronomical plates at the Harvard College Observatory plus converted blue band magnitudes from the collection of the Sternberg Observatory.

Table 6.4 summarizes the visual magnitudes from the AAVSO.

Table 6.5 contains photographic visual magnitudes collected by the author at Harvard Observatory.

Table 6.1: Estimated values for BC Cyg at its faintest and brightest

B	B-V	V	$M_V$	$(B - V)_0$	BC	$m_{bol}$
13.04	3.105	9.935	-4.97	1.785	-2.97	-7.94
12.54	3.052	9.488	-5.45	1.730	-1.92	-7.47

Table 6.2: Blue band data from the collection of the Sternberg Observatory

HJD	B	HJD	B	HJD	B
2413452.3590	13.20	2435012.3610	13.20	2447733.3460	12.00
2413479.2820	13.30	2435041.2070	13.50	2447734.3600	12.05
2413836.4420	12.70	2435041.2320	13.30	2447735.4510	12.20
2413840.4160	12.40	2435334.4200	13.40	2447736.4880	12.08
2413842.4030	12.52	2435335.3310	13.10	2447737.3700	11.88
2414422.3950	12.74	2435336.4670	12.90	2447737.3990	12.18
2414431.3960	13.50	2435337.3300	12.72	2447740.5080	12.00
2414582.2730	12.72	2435341.4550	13.05	2447745.4990	12.32
2414602.1670	12.85	2435347.3910	12.68	2447746.5250	12.32
2414928.2690	13.20	2435347.4170	12.75	2447747.4750	12.05
2415310.2450	13.60	2435361.3290	12.70	2447748.3380	12.00
2416734.3080	12.60	2435362.3110	12.70	2447749.4300	12.45
2417825.2960	13.50	2435362.3380	12.73	2447766.3920	12.05
2417850.2540	13.12	2435363.3220	12.80	2447768.3910	11.95
2417854.3210	13.15	2435365.2940	12.80	2447773.3460	12.00
2418240.2150	12.50	2435366.3260	13.10	2447774.3350	11.92
2424684.2100	12.95	2435367.3530	12.85	2447776.3800	11.92
2428654.4730	11.96	2435369.2970	12.93	2447777.3840	11.92
2429159.3090	11.95	2435369.3220	12.92	2447778.4280	11.92
2429161.2850	12.00	2435395.2380	13.20	2447779.3950	11.89
2429162.2650	11.95	2435401.3910	12.90	2447789.2250	11.65
2429167.2890	12.00	2435723.3650	12.85	2447791.2620	11.90
2429168.3130	12.05	2436084.3880	12.76	2447792.3240	11.83
2429170.2430	12.05	2436100.3090	12.80	2447793.3090	11.87
2429395.4490	13.05	2436128.3170	12.80	2447797.3020	12.08
2429485.4010	13.20	2436134.3080	13.00	2447798.3780	11.97
2429488.3680	13.30	2436805.3240	13.12	2447802.2860	11.97
2429491.3800	13.32	2438299.3200	13.50	2447803.3230	11.94
2429496.4110	13.30	2438466.5300	13.40	2447805.2720	11.88
2429496.4370	13.10	2443806.2480	12.20	2447807.3490	11.92
2429497.3830	13.50	2443806.2770	12.80	2447808.3720	11.98
2430585.3510	12.65	2443806.3000	12.05	2447821.2610	11.85
2430585.3740	12.85	2447680.5050	13.05	2447821.2960	11.92
2430587.3340	12.70	2447681.4830	12.75	2447821.3340	11.87
2430587.3580	12.70	2447681.4930	12.72	2447825.3240	11.92
2430592.2800	12.73	2447683.3350	12.60	2447829.2550	11.85
2430592.3160	12.70	2447683.3590	12.75	2447835.2050	12.03
2434239.3100	13.18	2447683.3860	12.70	2448119.4510	12.90
2434328.3440	13.15	2447683.4140	12.76	2448122.4240	13.04
2434330.1860	13.35	2447683.4390	12.76	2448124.4290	13.00
2434331.1890	13.70	2447683.4660	12.76	2448128.3830	12.88
2434333.1770	13.50	2447683.4940	12.72	2448132.4470	12.80
2434477.5110	13.40	2447704.3310	12.75	2448153.3600	12.90
2434480.4630	13.80	2447705.3160	12.72	2448453.4790	12.29
2434623.2620	13.00	2447706.3240	12.60	2448475.4380	12.34
2434678.2370	12.60	2447707.3180	12.36	2448484.4180	12.20
2434683.2270	13.40	2447707.3450	12.50	2448814.3610	13.00
2434869.4480	13.10	2447710.4890	12.35	2448864.3440	13.35
2434978.3650	13.30	2447711.3140	12.50	2448886.3460	13.42
2434980.3930	12.85	2447716.4970	12.52	2448899.3420	13.40
2434980.4590	13.65	2447717.4500	12.22	2448916.2350	13.42

HJD	B
2449570.4340	13.40
2449573.4460	13.35
2449601.3690	13.32
2449629.2530	13.32
2449892.4580	12.34
2449903.4900	12.37
2449931.4260	12.72
2449934.4260	12.80
2450014.2350	12.80
2450284.4370	13.10

Table 6.3: Blue estimates from Harvard College Observatory plus converted blue band data from Sternberg Observatory.

HJD	B	HJD	B	HJD	B
2411584.7000	13.20	2416412.5330	12.80	2420384.5776	13.50
2412352.6050	12.80	2416420.5353	13.00	2420385.5880	13.40
2412359.5726	12.70	2416444.4724	12.90	2420390.6228	13.20
2412378.5977	12.60	2416461.4667	12.50	2420395.5634	12.90
2412679.7060	12.50	2416552.8968	12.70	2420460.4549	13.40
2412790.4290	13.60	2416556.8900	12.40	2420601.7732	13.40
2412993.8099	13.00	2416603.8333	12.40	2420833.5294	13.20
2413078.5827	12.80	2416617.7916	13.00	2421051.7732	13.20
2413155.4637	13.10	2416664.7415	13.00	2421105.7106	13.20
2413300.8556	12.60	2416680.8706	12.90	2421106.6116	13.20
2413385.7265	13.20	2416692.7041	12.90	2421128.5954	13.20
2413441.6041	13.00	2416693.7245	13.20	2421436.7035	13.00
2413450.7120	13.10	2416719.6275	12.70	2421519.4922	13.20
2413452.3590	13.05	2416733.0767	12.80	2421840.6054	13.00
2413479.2820	13.12	2416734.3080	12.65	2423637.4074	12.80
2413789.5471	12.50	2416754.5693	12.80	2423649.3133	12.70
2413836.4420	12.72	2416761.5867	12.80	2423649.3836	12.80
2413840.4160	12.52	2416771.5811	12.70	2423696.2417	13.00
2413842.4030	12.60	2416793.5420	12.60	2423723.2254	12.80
2413864.5645	12.60	2416794.5338	12.80	2423738.5152	12.80
2414189.6522	12.70	2416800.5235	12.80	2423899.8355	13.00
2414422.3950	12.74	2416817.4689	12.70	2423986.6740	13.20
2414431.3960	13.26	2416821.4657	12.70	2424000.6887	13.10
2414564.5576	12.30	2416966.7876	12.80	2424256.8535	12.40
2414582.2730	12.73	2416967.8376	12.90	2424288.8020	12.70
2414602.1670	12.82	2417053.7074	13.10	2424307.7751	12.70
2414643.4521	13.00	2417126.5564	12.80	2424334.7775	12.60
2414798.7889	12.80	2417145.4658	12.90	2424335.7737	12.40
2414799.7839	13.20	2417405.8368	13.00	2424362.5846	13.00
2414831.7736	12.80	2417523.5703	13.20	2424364.6271	12.70
2414928.2690	13.05	2417529.5658	12.50	2424380.6337	12.70
2415210.7257	12.40	2417564.4789	13.00	2424391.5426	12.40
2415310.2450	13.32	2417739.7528	12.70	2424420.5776	12.50
2415313.6238	13.30	2417825.2960	13.26	2424441.5152	12.50
2415634.5845	12.70	2417850.2540	13.00	2424476.4697	12.80
2415666.5625	13.80	2417854.3210	13.02	2424670.7657	13.20
2415693.4450	13.20	2418095.6838	13.20	2424684.2100	12.89
2415710.4769	13.80	2418119.6196	12.80	2424697.7801	13.20
2415928.7938	12.90	2418218.5950	12.80	2424709.7180	13.50
2415941.7720	13.00	2418227.6254	13.10	2424770.5954	13.10
2416030.5822	13.00	2418240.2150	12.58	2424808.5510	12.80
2416033.5505	13.20	2418290.4495	12.80	2424812.5385	13.10
2416033.6187	12.80	2418617.5285	12.70	2424831.4611	12.90
2416055.5405	12.80	2418637.4928	12.70	2424973.8570	12.80
2416061.5111	13.10	2418641.4456	12.70	2424994.8489	13.00
2416259.8273	12.70	2418925.5977	12.10	2425039.7867	12.70
2416386.5554	13.10	2418937.6887	12.90	2425066.7344	12.90
2416387.6063	12.90	2419263.6776	12.70	2425096.6156	12.80
2416394.5605	13.20	2419269.7357	13.00	2425098.6449	13.00
2416394.5955	12.90	2419292.5843	12.80	2425128.5592	12.90
2416401.6238	12.80	2419694.4780	12.80	2425147.5587	13.00

HJD	B	HJD	B	HJD	B
2425204.4752	12.90	2426547.7312	12.70	2428749.6842	12.90
2425354.8554	13.00	2426549.7117	12.90	2428786.5856	12.80
2425374.7692	13.10	2426592.6437	12.90	2428814.5486	13.00
2425410.7134	13.00	2426593.6375	13.10	2428832.5123	12.90
2425443.7097	13.10	2426595.6292	12.80	2428873.4729	12.90
2425522.6025	13.30	2426603.6035	12.80	2429015.8321	12.80
2425535.5223	12.90	2426609.5881	13.10	2429071.8021	12.60
2425557.4811	12.90	2426615.5825	12.80	2429079.7825	12.60
2425602.4703	12.70	2426653.5194	12.90	2429082.7212	12.50
2425729.8129	12.90	2426838.8274	13.20	2429084.7385	12.60
2425745.8045	12.40	2426901.5984	13.40	2429086.7380	12.20
2425764.8094	12.80	2426917.6554	13.40	2429105.6580	12.50
2425775.7282	12.50	2426957.5631	13.00	2429159.3090	12.21
2425790.7736	12.80	2426979.5874	12.80	2429161.2850	12.25
2425792.7389	12.60	2426984.5412	12.40	2429162.2650	12.21
2425795.7768	12.70	2427002.5556	13.00	2429165.5365	12.20
2425796.7701	12.60	2427215.7333	12.70	2429167.2890	12.25
2425800.7460	12.40	2427327.5528	13.20	2429168.3130	12.28
2425801.7798	12.70	2427329.5302	13.00	2429170.2430	12.28
2425805.7824	12.50	2427335.5536	13.00	2429170.5361	12.30
2425807.8287	12.40	2427346.5368	13.10	2429179.4932	12.40
2425809.6120	12.40	2427366.4751	13.20	2429213.4931	12.30
2425822.7469	12.70	2427378.5257	13.10	2429223.4975	12.60
2425823.7151	12.70	2427392.5226	13.20	2429384.8266	12.60
2425824.7337	12.70	2427397.4611	13.00	2429395.4490	12.95
2425825.7288	12.60	2427397.5225	13.30	2429433.7355	12.80
2425825.7842	12.20	2427600.7704	13.10	2429455.7097	13.10
2425830.7171	12.20	2427602.7478	13.00	2429457.7433	12.80
2425831.6813	12.50	2427641.6831	13.00	2429483.7103	13.00
2425831.7447	12.40	2427657.6901	12.80	2429485.4010	13.05
2425840.6031	12.40	2427658.6517	12.90	2429488.3680	13.12
2425870.6614	12.80	2427664.6501	13.00	2429491.3800	13.13
2425874.5544	12.90	2427668.6494	12.80	2429491.5909	13.10
2425878.5895	12.70	2427670.6608	12.80	2429496.4110	13.12
2425879.6292	12.80	2427681.6731	13.20	2429496.4370	12.99
2425889.5956	12.50	2427713.5036	13.00	2429497.3830	13.26
2425893.5498	12.70	2427744.5317	12.90	2429509.5715	13.00
2425895.5437	12.70	2427764.4798	12.90	2429511.5547	13.20
2425910.4860	13.20	2427953.7807	12.90	2429514.5878	13.20
2425921.4767	12.80	2427977.7835	12.80	2429518.5286	13.30
2425925.4681	13.00	2427984.6462	12.40	2429522.5220	13.40
2425937.4834	13.10	2428021.6671	13.20	2429523.5619	13.30
2426095.7911	13.60	2428033.7316	13.00	2429551.4895	13.20
2426172.6465	13.00	2428066.5409	13.00	2429801.8096	13.00
2426183.7024	13.00	2428092.5078	13.10	2429804.7954	12.70
2426187.6223	12.90	2428347.6221	12.70	2429808.7815	12.70
2426188.6530	13.00	2428356.7254	12.70	2429816.7210	12.80
2426190.6879	13.10	2428381.6653	12.80	2429817.7577	12.60
2426191.7073	13.00	2428399.6425	12.80	2429821.7439	12.70
2426205.6596	13.00	2428643.8454	12.40	2429845.6381	12.70
2426207.7059	13.30	2428654.4730	12.22	2429845.6909	12.80
2426209.6844	13.20	2428669.8044	12.90	2429850.6659	12.80
2426300.4679	12.90	2428722.7159	12.90	2429869.5736	12.90
2426307.4913	12.90	2428722.7975	12.80	2429876.5958	12.80

HJD	B	HJD	B	HJD	B
2429903.5249	12.80	2431329.6362	12.90	2431701.5675	13.00
2429908.5200	12.80	2431341.5279	13.00	2431701.5708	12.80
2429910.5157	12.80	2431341.5979	12.80	2431701.7019	12.90
2429921.4842	12.80	2431342.6721	12.90	2431702.5434	12.80
2429926.4731	12.80	2431343.6265	12.80	2431707.5452	12.90
2430092.8475	12.80	2431344.5338	12.80	2431707.5599	12.90
2430186.7364	13.00	2431349.6389	12.80	2431707.6395	12.80
2430258.5311	13.20	2431350.6286	12.80	2431709.5579	12.90
2430526.7558	12.90	2431356.5988	12.80	2431711.5969	12.90
2430531.7727	12.80	2431356.6459	12.90	2431711.6385	12.90
2430548.7599	12.40	2431357.5733	12.80	2431712.5866	12.80
2430554.7251	12.90	2431357.6197	12.80	2431712.5887	12.90
2430585.3510	12.68	2431357.6640	12.90	2431729.5421	12.70
2430585.3740	12.82	2431359.5548	12.90	2431731.5825	12.70
2430587.3340	12.72	2431367.5185	12.80	2431756.5247	12.70
2430587.3580	12.72	2431375.4909	12.90	2431757.5027	12.80
2430592.2800	12.74	2431375.5346	12.90	2431759.4967	12.80
2430592.3160	12.72	2431375.5830	12.70	2431811.4664	12.80
2430604.5736	12.80	2431375.6287	12.70	2431813.4632	12.80
2430616.5503	13.00	2431378.5204	12.90	2432030.6680	12.40
2430643.5594	12.80	2431378.5703	12.80	2432064.6923	12.20
2430996.5463	13.20	2431379.5143	12.80	2432084.5442	12.30
2431028.4936	12.90	2431380.5380	12.80	2432168.4852	12.40
2431227.7720	12.80	2431382.5320	12.70	2432170.4888	12.50
2431230.7914	12.80	2431383.7153	12.70	2432353.7725	13.10
2431230.8075	12.80	2431386.4979	12.70	2432365.7740	12.80
2431231.7802	12.90	2431398.5223	12.70	2432391.7676	12.90
2431236.7646	12.90	2431399.4909	12.70	2432468.6502	12.80
2431268.6833	12.90	2431638.7877	13.00	2432728.6976	12.30
2431281.6332	12.80	2431640.5870	13.00	2432729.6300	12.20
2431281.7488	12.80	2431640.7145	13.10	2432731.6536	12.50
2431285.7084	12.80	2431643.5891	13.20	2432733.6817	12.30
2431293.6996	13.10	2431643.7131	13.20	2432734.7782	12.60
2431303.5886	12.80	2431644.5850	13.00	2432735.7714	12.40
2431303.6094	12.80	2431647.6806	13.20	2432736.6146	12.30
2431303.6302	13.00	2431647.7997	13.00	2432737.6831	12.20
2431303.6447	13.00	2431648.5871	12.90	2432740.6700	12.70
2431303.6586	13.00	2431649.5754	13.00	2432741.6105	12.40
2431303.6703	12.90	2431667.5574	13.00	2432742.6659	12.30
2431308.5681	13.00	2431671.5742	13.00	2432743.7158	12.80
2431311.5884	13.10	2431672.6352	13.00	2425410.7134	13.00
2431311.6708	13.10	2431672.7086	13.00	2425443.7097	13.10
2431311.7435	13.00	2431673.5674	12.90	2425522.6025	13.30
2431312.6106	13.00	2431673.7121	13.00	2425535.5223	12.90
2431312.7499	13.00	2431677.6588	12.80	2425557.4811	12.90
2431318.5654	12.90	2431678.5636	13.10	2425602.4703	12.70
2431318.6211	12.90	2431683.5521	12.90	2425729.8129	12.90
2431318.7787	13.00	2431683.5951	12.90	2425745.8045	12.40
2431321.5919	13.10	2431683.6744	12.90	2425764.8094	12.80
2431321.6446	13.10	2431684.5529	12.90	2425775.7282	12.50
2431321.6670	12.80	2431684.5896	12.80	2425790.7736	12.80
2431322.5960	13.00	2431685.5565	12.80	2425792.7389	12.60
2431323.5762	12.90	2431686.6805	12.90	2425795.7768	12.70
2431323.6572	12.90	2431686.6909	12.90	2425796.7701	12.60

HJD	B	HJD	B	HJD	B
2425801.7798	12.70	2427329.5302	13.00	2429170.2430	12.28
2425805.7824	12.50	2427335.5536	13.00	2429170.5361	12.30
2425807.8287	12.40	2427346.5368	13.10	2429179.4932	12.40
2425809.6120	12.40	2427366.4751	13.20	2429213.4931	12.30
2425822.7469	12.70	2427378.5257	13.10	2429223.4975	12.60
2425823.7151	12.70	2427392.5226	13.20	2429384.8266	12.60
2425824.7337	12.70	2427397.4611	13.00	2429395.4490	12.95
2425825.7288	12.60	2427397.5225	13.30	2429433.7355	12.80
2425825.7842	12.20	2427600.7704	13.10	2429455.7097	13.10
2425830.7171	12.20	2427602.7478	13.00	2429457.7433	12.80
2425831.6813	12.50	2427641.6831	13.00	2429483.7103	13.00
2425831.7447	12.40	2427657.6901	12.80	2429485.4010	13.05
2425840.6031	12.40	2427658.6517	12.90	2429488.3680	13.12
2425870.6614	12.80	2427664.6501	13.00	2429491.3800	13.13
2425874.5544	12.90	2427668.6494	12.80	2429491.5909	13.10
2425878.5895	12.70	2427670.6608	12.80	2429496.4110	13.12
2425879.6292	12.80	2427681.6731	13.20	2429496.4370	12.99
2425889.5956	12.50	2427713.5036	13.00	2429497.3830	13.26
2425893.5498	12.70	2427744.5317	12.90	2429509.5715	13.00
2425895.5437	12.70	2427764.4798	12.90	2429511.5547	13.20
2425910.4860	13.20	2427953.7807	12.90	2429514.5878	13.20
2425921.4767	12.80	2427977.7835	12.80	2429518.5286	13.30
2425925.4681	13.00	2427984.6462	12.40	2429522.5220	13.40
2425937.4834	13.10	2428021.6671	13.20	2429523.5619	13.30
2426095.7911	13.60	2428033.7316	13.00	2429551.4895	13.20
2426172.6465	13.00	2428066.5409	13.00	2429801.8096	13.00
2426183.7024	13.00	2428092.5078	13.10	2429804.7954	12.70
2426187.6223	12.90	2428347.6221	12.70	2429808.7815	12.70
2426188.6530	13.00	2428356.7254	12.70	2429816.7210	12.80
2426190.6879	13.10	2428381.6653	12.80	2429817.7577	12.60
2426191.7073	13.00	2428399.6425	12.80	2429821.7439	12.70
2426205.6596	13.00	2428643.8454	12.40	2429845.6381	12.70
2426207.7059	13.30	2428654.4730	12.22	2429845.6909	12.80
2426209.6844	13.20	2428669.8044	12.90	2429850.6659	12.80
2426300.4679	12.90	2428722.7159	12.90	2429869.5736	12.90
2426307.4913	12.90	2428722.7975	12.80	2429876.5958	12.80
2426471.7974	12.50	2428724.7240	12.90	2429883.5830	12.80
2426547.7312	12.70	2428749.6842	12.90	2429903.5249	12.80
2426549.7117	12.90	2428786.5856	12.80	2429908.5200	12.80
2426592.6437	12.90	2428814.5486	13.00	2429910.5157	12.80
2426593.6375	13.10	2428832.5123	12.90	2429921.4842	12.80
2426595.6292	12.80	2428873.4729	12.90	2429926.4731	12.80
2426603.6035	12.80	2429015.8321	12.80	2430092.8475	12.80
2426609.5881	13.10	2429071.8021	12.60	2430186.7364	13.00
2426615.5825	12.80	2429079.7825	12.60	2430258.5311	13.20
2426653.5194	12.90	2429082.7212	12.50	2430526.7558	12.90
2426838.8274	13.20	2429084.7385	12.60	2430531.7727	12.80
2426901.5984	13.40	2429086.7380	12.20	2430548.7599	12.40
2426917.6554	13.40	2429105.6580	12.50	2430554.7251	12.90
2426957.5631	13.00	2429159.3090	12.21	2430585.3510	12.68
2426979.5874	12.80	2429161.2850	12.25	2430585.3740	12.82
2426984.5412	12.40	2429162.2650	12.21	2430587.3340	12.72
2427002.5556	13.00	2429165.5365	12.20	2430587.3580	12.72
2427215.7333	12.70	2429167.2890	12.25	2430592.2800	12.74

HJD	B	HJD	B	HJD	B
2430604.5736	12.80	2431375.6287	12.70	2432803.5427	12.60
2430616.5503	13.00	2431378.5204	12.90	2432827.5324	12.60
2430643.5594	12.80	2431378.5703	12.80	2432828.5936	12.60
2430996.5463	13.20	2431379.5143	12.80	2433090.7446	12.90
2431028.4936	12.90	2431380.5380	12.80	2433155.5769	12.80
2431227.7720	12.80	2431382.5320	12.70	2433203.5246	12.70
2431230.7914	12.80	2431383.7153	12.70	2433210.5069	12.30
2431230.8075	12.80	2431386.4979	12.70	2433210.5736	12.30
2431231.7802	12.90	2431398.5223	12.70	2433236.4990	12.40
2431236.7646	12.90	2431399.4909	12.70	2433448.7539	12.20
2431268.6833	12.90	2431638.7877	13.00	2433458.7780	12.50
2431281.6332	12.80	2431640.5870	13.00	2433470.7439	12.50
2431281.7488	12.80	2431640.7145	13.10	2433471.6642	12.20
2431285.7084	12.80	2431643.5891	13.20	2433805.7777	13.10
2431293.6996	13.10	2431643.7131	13.20	2433835.7657	13.10
2431303.5886	12.80	2431644.5850	13.00	2433840.7349	13.20
2431303.6094	12.80	2431647.6806	13.20	2433861.6748	13.10
2431303.6302	13.00	2431647.7997	13.00	2433864.7248	13.20
2431303.6447	13.00	2431648.5871	12.90	2433882.6114	13.00
2431303.6586	13.00	2431649.5754	13.00	2433882.6415	13.10
2431303.6703	12.90	2431667.5574	13.00	2433932.5134	12.70
2431308.5681	13.00	2431671.5742	13.00	2434183.7380	12.80
2431311.5884	13.10	2431672.6352	13.00	2434207.7206	12.90
2431311.6708	13.10	2431672.7086	13.00	2434239.3100	13.04
2431311.7435	13.00	2431673.5674	12.90	2434263.5849	13.00
2431312.6106	13.00	2431673.7121	13.00	2434264.5420	12.80
2431312.7499	13.00	2431677.6588	12.80	2434328.3440	13.02
2431318.5654	12.90	2431678.5636	13.10	2434330.1860	13.15
2431318.6211	12.90	2431683.5521	12.90	2434331.1890	13.39
2431318.7787	13.00	2431683.5951	12.90	2434333.1770	13.26
2431321.5919	13.10	2431683.6744	12.90	2434477.5110	13.19
2431321.6446	13.10	2431684.5529	12.90	2434480.4630	13.46
2431321.6670	12.80	2431684.5896	12.80	2434623.2620	12.92
2431322.5960	13.00	2431685.5565	12.80	2434678.2370	12.65
2431323.5762	12.90	2431686.6805	12.90	2434683.2270	13.19
2431323.6572	12.90	2431686.6909	12.90	2434869.4480	12.99
2431329.5614	12.90	2431687.6972	12.80	2434978.3650	13.12
2431329.6362	12.90	2431701.5675	13.00	2434980.3930	12.82
2431341.5279	13.00	2431701.5708	12.80	2434980.4590	13.36
2431341.5979	12.80	2431701.7019	12.90	2434982.3650	13.12
2431342.6721	12.90	2431702.5434	12.80	2434982.4160	13.12
2431343.6265	12.80	2431707.5452	12.90	2435006.3740	13.13
2431344.5338	12.80	2431707.5599	12.90	2435011.3400	13.29
2431349.6389	12.80	2431707.6395	12.80	2435012.3610	13.05
2431350.6286	12.80	2431709.5579	12.90	2435041.2070	13.26
2431356.5988	12.80	2431711.5969	12.90	2435041.2320	13.12
2431356.6459	12.90	2431711.6385	12.90	2435334.4200	13.19
2431357.5733	12.80	2431712.5866	12.80	2435335.3310	12.99
2431357.6197	12.80	2431712.5887	12.90	2435336.4670	12.85
2431357.6640	12.90	2431729.5421	12.70	2435337.3300	12.73
2431359.5548	12.90	2431731.5825	12.70	2435341.4550	12.95
2431367.5185	12.80	2431756.5247	12.70	2435347.3910	12.70
2431375.4909	12.90	2431757.5027	12.80	2435347.4170	12.75
2431375.5346	12.90	2432747.7626	12.70	2435361.3290	12.72

HJD	B	HJD	B	HJD	B
2435362.3380	12.74	2442611.7830	12.80	2444543.5610	12.20
2435363.3220	12.78	2442634.6790	13.00	2444761.7710	12.90
2435365.2940	12.78	2442655.8360	13.40	2444783.7570	12.90
2435366.3260	12.99	2442659.6050	12.40	2444819.6720	13.10
2435367.3530	12.82	2442666.7720	13.00	2444837.5870	13.30
2435369.2970	12.87	2442694.5170	12.80	2444868.6040	12.70
2435369.3220	12.87	2442710.5190	13.00	2444899.5080	13.30
2435395.2380	13.05	2442714.4870	12.50	2444934.4730	12.90
2435401.3910	12.85	2442934.7850	12.70	2445082.8000	12.50
2435723.3650	12.82	2442952.7220	12.20	2445083.8160	12.50
2436084.3880	12.76	2442965.7060	12.30	2445141.7670	12.50
2436100.3090	12.78	2442982.6790	12.30	2445165.7180	12.00
2436128.3170	12.78	2442992.7640	12.10	2445173.7200	12.40
2436134.3080	12.92	2443010.6400	12.20	2445203.6620	12.20
2436805.3240	13.00	2443020.6520	12.20	2445223.6250	12.00
2437849.7113	12.80	2443041.6500	12.10	2445232.5520	12.20
2437851.7214	12.50	2443050.6610	12.20	2445253.6120	12.20
2437873.6500	12.90	2443063.5140	12.20	2445260.5260	12.10
2437873.6600	12.80	2443096.4610	12.00	2445281.5190	12.00
2438200.6910	12.40	2443135.4660	12.30	2445312.4790	12.20
2438202.6125	12.30	2443289.7910	12.60	2445317.4590	12.20
2438299.3200	13.26	2443307.7730	12.80	2445342.5080	12.20
2438466.5300	13.19	2443317.7800	12.60	2445438.8510	12.40
2440067.6850	12.40	2443334.7910	12.70	2445464.8150	12.60
2440395.7687	12.60	2443347.7010	13.10	2445496.7960	12.70
2440417.7079	12.60	2443366.6630	12.80	2445519.7410	13.10
2440418.7190	12.80	2443376.7250	13.00	2445525.6900	13.00
2440448.6302	12.80	2443395.6180	12.90	2445550.7210	12.90
2440452.6193	12.90	2443421.5780	13.00	2445556.6960	13.00
2440774.7376	12.10	2443449.5380	12.80	2445579.6470	13.10
2440775.7348	12.20	2443489.4680	12.80	2445587.5990	13.20
2440824.5975	12.20	2443659.7940	12.10	2445606.5830	12.90
2441181.6199	12.80	2443690.7200	12.10	2445614.5360	13.10
2441899.7050	13.10	2443716.6860	12.00	2445637.5200	13.00
2441900.6930	13.10	2443753.6590	12.00	2445646.4900	12.80
2441915.7050	13.20	2443776.5740	12.20	2445670.4710	12.80
2441943.5460	13.20	2443791.6840	12.00	2445694.4720	13.00
2441957.6130	13.10	2443806.2480	12.38	2445699.4440	12.40
2441971.5090	13.30	2443806.2770	12.78	2445728.4660	12.90
2441983.5000	13.20	2443806.3000	12.28	2445760.9180	12.60
2442211.7380	12.20	2443815.5240	12.20	2445786.8810	12.80
2442217.7980	12.20	2443838.4620	12.40	2445823.8190	12.30
2442219.7950	12.10	2444024.7930	12.70	2445823.8430	12.50
2442220.7940	12.10	2444045.7730	13.10	2445848.7840	12.20
2442248.7590	12.10	2444102.6800	13.10	2445855.7780	12.40
2442272.6600	12.20	2444128.5550	12.80	2445878.7970	12.20
2442303.5380	13.00	2444140.6220	12.90	2445884.6950	12.30
2442328.5910	12.60	2444197.4730	12.40	2445906.6960	12.10
2442362.4720	12.20	2444401.7770	12.30	2445910.6660	12.30
2442386.4560	12.20	2444439.7320	12.30	2445933.6460	12.10
2442397.4560	12.60	2444467.6670	12.20	2445938.6340	12.30
2442541.7700	12.90	2444486.6070	12.20	2445961.6210	12.30
2442543.8160	12.70	2444494.6610	12.00	2445989.5450	12.40
2442544.7830	12.90	2444513.5990	12.40	2446019.5320	12.30

HJD	B	HJD	B	HJD	B
2446061.5300	12.20	2447324.7060	12.70	2447776.3800	12.19
2446079.4860	12.20	2447330.7650	13.00	2447777.3840	12.19
2446124.9000	12.60	2447353.7510	12.90	2447778.4280	12.19
2446139.8620	12.70	2447378.6300	12.70	2447779.3950	12.17
2446180.8380	13.00	2447383.7370	12.30	2447789.2250	12.01
2446206.7890	13.00	2447411.5930	12.50	2447791.2620	12.18
2446231.7930	12.90	2447441.5740	12.50	2447792.3240	12.13
2446237.7400	12.90	2447466.5220	13.20	2447793.3090	12.16
2446264.7270	12.70	2447480.4890	12.80	2447797.3020	12.30
2446270.7270	13.00	2447497.4830	13.20	2447797.5270	12.10
2446287.7150	12.80	2447505.4850	13.00	2447798.3780	12.23
2446295.6420	13.00	2447628.8380	13.10	2447802.2860	12.23
2446316.6550	13.00	2447680.5050	12.95	2447803.3230	12.21
2446325.6610	13.10	2447681.4830	12.75	2447805.2720	12.17
2446345.6280	13.20	2447681.4930	12.73	2447807.3490	12.19
2446355.5270	13.20	2447683.3350	12.65	2447808.3720	12.23
2446378.5030	13.20	2447683.3590	12.75	2447821.2610	12.15
2446414.5130	13.30	2447683.3860	12.72	2447821.2960	12.19
2446435.4520	12.90	2447683.4140	12.76	2447821.3340	12.16
2446523.8850	12.20	2447683.4390	12.76	2447823.5920	12.20
2446534.8640	12.30	2447683.4660	12.76	2447825.3240	12.19
2446560.7870	12.60	2447683.4940	12.73	2447829.2550	12.15
2446565.8150	12.20	2447689.7580	12.60	2447835.2050	12.27
2446585.8020	12.40	2447704.3310	12.75	2448119.4510	12.85
2446590.8110	12.30	2447705.3160	12.73	2448122.4240	12.95
2446615.7200	12.50	2447706.3240	12.65	2448124.4290	12.92
2446622.7890	12.30	2447707.3180	12.49	2448128.3830	12.84
2446646.7960	12.70	2447707.3450	12.58	2448132.4470	12.78
2446651.7030	12.30	2447710.4890	12.48	2448153.3600	12.85
2446671.5920	12.70	2447711.3140	12.58	2448453.4790	12.44
2446681.5730	12.60	2447716.4970	12.60	2448475.4380	12.47
2446698.6380	12.70	2447716.7620	12.80	2448484.4180	12.38
2446709.5470	12.70	2447717.4500	12.39	2448814.3610	12.92
2446726.5260	12.70	2447718.4540	12.50	2448864.3440	13.15
2446733.5250	12.80	2447729.3190	12.60	2448886.3460	13.20
2446757.4980	13.00	2447730.2950	12.55	2448899.3420	13.19
2446769.4900	12.80	2447732.3750	12.31	2448916.2350	13.20
2446788.5070	12.50	2447733.3460	12.25	2449156.4170	12.52
2446915.8360	12.50	2447734.3600	12.28	2449163.4670	12.73
2446946.7980	12.30	2447735.4510	12.38	2449189.4340	12.50
2446970.7980	12.80	2447736.4880	12.30	2449241.3390	12.77
2446975.7350	12.20	2447736.7300	12.20	2449249.4580	12.78
2446999.7640	12.60	2447737.3700	12.17	2449271.2340	12.77
2447005.6900	12.40	2447737.3990	12.37	2449281.2910	12.92
2447028.6440	12.60	2447740.5080	12.25	2449570.4340	13.19
2447033.6230	12.30	2447745.4990	12.46	2449573.4460	13.15
2447064.6460	12.60	2447746.5250	12.46	2449601.3690	13.13
2447082.6140	12.70	2447747.4750	12.28	2449629.2530	13.13
2447087.5750	12.30	2447748.3380	12.25	2449892.4580	12.47
2447112.5590	12.70	2447749.4300	12.55	2449903.4900	12.50
2447148.4980	12.70	2447762.6660	12.20	2449931.4260	12.73
2447167.4570	12.50	2447766.3920	12.28	2449934.4260	12.78
2447237.8900	12.70	2447768.3910	12.21	2450014.2350	12.78
2447270.8350	13.00	2447773.3460	12.25	2450284.4370	12.99

Table 6.4: Visual observations from the AAVSO

HJD	V	HJD	V	HJD	V
2433264.5000	09.80	2440725.0000	10.70	2441992.7000	10.80
2433267.5000	09.60	2440740.8000	09.60	2441999.7000	10.70
2433283.5000	09.30	2440759.8000	10.00	2442006.7000	10.40
2433291.5000	09.40	2440772.7000	09.30	2442015.5000	10.50
2433570.8000	09.30	2440773.7000	10.70	2442018.7000	10.70
2433584.8000	09.60	2440797.7000	09.80	2442024.7000	10.40
2433854.6000	09.40	2440804.6000	09.30	2442027.6000	10.60
2433860.6000	10.50	2440830.7000	10.40	2442041.6000	10.10
2433910.6000	10.60	2440838.8000	10.00	2442057.6000	10.20
2433924.6000	10.00	2440878.7000	09.50	2442163.0000	10.50
2433941.6000	10.10	2440886.7000	09.50	2442166.0000	09.70
2433945.6000	09.60	2440896.6000	09.40	2442186.9000	09.80
2435186.8000	09.80	2440949.7000	09.50	2442188.8000	09.80
2435197.8000	10.30	2441030.8000	09.80	2442199.8000	09.70
2435208.8000	10.50	2441045.9000	10.70	2442207.9000	10.00
2435245.6000	10.60	2441077.9000	10.80	2442211.8000	09.40
2435388.7000	10.30	2441114.8000	10.30	2442214.8000	10.10
2439658.8000	09.80	2441121.7000	09.50	2442225.8000	09.70
2439699.8000	09.70	2441148.7000	10.90	2442226.9000	09.20
2439729.7000	10.10	2441177.7000	10.90	2442237.8000	09.70
2439755.9000	09.90	2441190.7000	10.50	2442247.7000	09.60
2439795.7000	10.00	2441206.6000	10.60	2442269.7000	09.70
2439851.7000	10.00	2441235.7000	10.80	2442294.7000	09.60
2439941.9000	10.90	2441244.7000	10.60	2442326.8000	09.70
2439977.8000	10.10	2441245.8000	10.60	2442345.7000	09.70
2440029.7000	10.00	2441250.6000	10.20	2442358.7000	09.80
2440036.8000	10.00	2441256.7000	10.60	2442390.7000	09.90
2440043.7000	09.60	2441273.7000	10.60	2442393.5000	10.00
2440056.8000	10.00	2441276.6000	11.00	2442584.8000	10.00
2440073.6000	09.20	2441286.6000	10.80	2442599.8000	10.70
2440115.8000	10.00	2441295.6000	10.50	2442631.7000	10.60
2440126.8000	10.00	2441316.6000	10.90	2442663.8000	10.70
2440154.7000	09.70	2441327.6000	10.70	2442690.7000	10.80
2440155.7000	09.10	2441423.8000	10.70	2442715.8000	10.80
2440174.7000	09.00	2441431.0000	10.60	2442726.7000	10.40
2440193.7000	08.50	2441447.8000	09.90	2442748.7000	10.90
2440266.9000	09.60	2441521.7000	10.50	2442771.7000	10.80
2440297.9000	10.30	2441522.7000	09.20	2442949.8000	10.70
2440322.8000	10.10	2441522.7000	10.10	2442983.7000	10.10
2440355.8000	10.60	2441650.7000	09.30	2442994.7000	09.80
2440381.7000	10.70	2441763.9000	10.30	2443040.7000	09.90
2440386.8000	10.50	2441795.9000	10.60	2443075.7000	09.70
2440414.7000	10.00	2441805.8000	10.60	2443098.7000	09.70
2440436.6000	10.70	2441844.8000	10.00	2443121.6000	09.80
2440479.8000	10.90	2441857.7000	09.90	2443313.8000	10.10
2440506.8000	10.40	2441868.7000	10.90	2443332.8000	10.80
2440512.7000	10.70	2441897.7000	10.60	2443363.7000	10.90
2440531.7000	10.30	2441899.7000	10.70	2443404.6000	10.90
2440548.7000	10.50	2441927.7000	11.30	2443439.7000	11.10
2440582.5000	09.90	2441941.8000	10.20	2443460.7000	10.80
2440592.7000	10.70	2441952.7000	10.20	2443658.8000	10.70
2440643.0000	10.70	2441964.7000	10.50	2443675.8000	10.10

HJD	V	HJD	V	HJD	V
2443793.7201	09.60	2445550.3000	10.00	2447065.3000	09.40
2443804.8000	08.80	2445558.3000	10.20	2447075.4000	09.40
2443819.7000	09.90	2445605.3000	10.30	2447086.3000	09.50
2443854.6000	09.70	2445610.3000	10.40	2447139.2000	09.40
2444090.4000	10.00	2445630.3000	10.00	2447159.2000	09.50
2444097.4000	10.40	2445643.3000	10.30	2447167.2000	09.50
2444131.3000	10.30	2445648.3000	10.20	2447352.4000	09.50
2444136.3000	10.20	2445658.2000	10.40	2447359.7000	09.40
2444143.3000	10.30	2445674.2000	10.30	2447361.4000	09.50
2444148.9000	10.20	2445867.5000	10.00	2447372.4000	09.50
2444155.3000	10.60	2445874.5000	10.30	2447412.3000	09.70
2444164.4000	10.20	2445890.3000	10.30	2447416.6000	09.70
2444174.2000	10.20	2445911.3000	09.90	2447426.3000	09.70
2444180.3000	10.40	2445923.4000	09.50	2447435.3000	09.60
2444187.2000	10.30	2445930.3000	09.50	2447446.3000	09.70
2444192.3000	10.20	2445965.3000	09.70	2447456.3000	09.70
2444196.2000	10.20	2445973.3000	09.50	2447466.2000	09.70
2444210.2000	10.20	2445986.3000	09.60	2447472.3000	10.20
2444444.4000	10.30	2445994.3000	09.70	2447473.5000	10.20
2444454.4000	09.50	2446005.3000	09.70	2447480.2000	10.10
2444467.3000	09.50	2446012.2000	09.40	2447480.6000	10.20
2444471.3000	10.10	2446040.2000	09.60	2447489.2000	10.70
2444501.3000	09.50	2446056.2000	09.30	2447503.2000	10.40
2444510.3000	09.70	2446244.4000	09.50	2447696.4000	10.40
2444516.3000	09.50	2446258.4000	09.70	2447704.4000	09.50
2444520.3000	09.50	2446271.4000	10.00	2447738.4000	09.60
2444532.2000	09.50	2446279.4000	10.10	2447775.3000	09.00
2444540.3000	09.50	2446319.3000	09.90	2447786.3000	09.00
2444567.3000	09.60	2446328.3000	09.90	2447794.3000	09.10
2444581.2000	09.50	2446335.3000	09.60	2447803.3000	09.10
2444600.2000	09.50	2446349.4000	10.10	2447810.3000	09.10
2444814.4000	09.30	2446359.3000	10.00	2447817.3000	09.00
2444821.4000	10.30	2446368.3000	10.20	2447824.3000	09.20
2444831.4000	10.40	2446376.3000	10.20	2447837.3400	09.10
2444871.3000	10.40	2446385.2000	10.10	2447846.3000	09.30
2444914.2000	10.50	2446401.2000	10.10	2447854.3000	09.10
2444929.2000	10.50	2446418.2000	10.10	2447859.3568	09.20
2444937.2000	10.50	2446423.2000	10.10	2447859.3568	09.00
2445158.4000	10.30	2446593.5881	10.10	2447859.3569	09.20
2445170.4000	09.50	2446616.4000	09.70	2447859.3711	09.00
2445178.3000	09.70	2446623.4000	09.60	2447859.3711	09.20
2445183.4000	09.50	2446639.4000	09.50	2447859.3712	09.40
2445193.4000	09.70	2446648.4000	10.00	2447859.3712	09.20
2445225.3000	09.50	2446652.4340	09.70	2447859.3712	09.30
2445233.4000	09.60	2446684.3000	10.10	2447859.4457	09.40
2445241.3000	09.90	2446694.3000	09.70	2447859.4457	09.40
2445269.4000	09.60	2446700.3000	09.90	2447859.4458	09.40
2445282.3000	09.40	2446707.3000	09.70	2447859.4600	09.40
2445294.3000	09.40	2446716.3000	09.90	2447859.4601	09.50
2445303.2000	09.30	2446730.3000	09.90	2447859.4601	09.90
2445327.2000	09.40	2446739.2000	09.90	2447859.4601	09.40
2445505.4000	09.60	2446746.2000	09.90	2447861.3000	09.40
2445524.4000	09.90	2446761.2000	09.90	2447870.2500	09.40
2445533.3000	10.20	2447047.3000	09.90	2447883.2400	09.50

HJD	V	HJD	V	HJD	V
2447891.8004	09.70	2447977.0966	09.00	2448153.3100	10.10
2447891.8004	09.80	2447977.0966	09.00	2448154.7804	10.30
2447891.8005	09.90	2447977.0968	09.50	2448154.7947	09.90
2447891.8892	09.70	2447977.1109	09.70	2448154.8692	10.30
2447891.8893	09.80	2447977.1109	09.80	2448154.8692	09.70
2447891.9782	09.90	2447977.1109	09.60	2448154.8834	09.00
2447912.1374	09.90	2447977.1111	09.80	2448154.8834	09.40
2447912.1374	09.50	2447977.1854	09.80	2448154.8835	09.00
2447912.1374	09.30	2447977.1855	09.70	2448154.8835	09.20
2447912.1517	09.30	2447977.1855	09.80	2448154.9724	09.20
2447912.1518	09.20	2447977.1857	09.90	2448154.9724	09.00
2447912.2263	09.30	2447977.1998	09.90	2448154.9724	09.00
2447912.2263	09.30	2447977.1998	09.90	2448162.3000	09.40
2447912.2263	09.30	2447977.1998	09.90	2448170.4100	09.00
2447912.2264	09.20	2447977.2000	09.80	2448170.4211	09.00
2447912.2406	09.30	2447977.2745	09.80	2448170.4211	09.30
2447912.2406	09.50	2447977.2888	09.90	2448170.4212	09.70
2447912.2406	09.30	2448031.5300	09.90	2448170.4354	09.20
2447912.2407	09.30	2448042.2273	09.80	2448170.4355	09.40
2447912.3152	09.30	2448042.3162	09.90	2448170.5099	09.70
2447912.3152	09.20	2448042.3305	09.90	2448170.5099	09.50
2447912.3152	09.30	2448042.4051	09.90	2448170.5100	09.30
2447912.3152	09.50	2448042.4194	10.00	2448170.5101	09.20
2447912.3153	09.20	2448047.4200	09.90	2448170.5243	09.50
2447912.3295	09.20	2448058.5000	09.90	2448170.5243	09.70
2447912.3295	09.30	2448062.8449	10.00	2448170.5243	09.60
2447912.3295	09.40	2448062.8593	09.20	2448170.5245	10.30
2447912.3296	09.30	2448062.9338	09.10	2448170.6133	09.60
2447956.2107	09.30	2448062.9482	09.00	2448181.3200	09.40
2447956.2107	09.40	2448072.4300	09.40	2448191.3400	09.80
2447956.2107	09.30	2448082.4500	09.50	2448200.3000	10.50
2447956.2108	09.80	2448089.4000	09.00	2448204.3551	09.50
2447956.2250	09.50	2448098.3000	09.10	2448204.3694	10.50
2447956.2250	09.90	2448102.8249	09.00	2448204.4438	09.50
2447956.2250	09.30	2448102.8993	09.50	2448204.4438	09.90
2447956.2252	09.30	2448102.8993	09.50	2448204.4438	09.10
2447956.2995	09.90	2448102.8993	09.10	2448204.4438	09.70
2447956.2996	09.50	2448102.8995	09.50	2448204.4440	10.00
2447956.2997	09.50	2448102.9136	09.30	2448204.4581	09.10
2447956.3139	09.60	2448102.9136	09.40	2448204.4581	10.10
2447956.3139	09.90	2448102.9138	09.50	2448204.4582	09.70
2447956.3139	09.90	2448105.3800	09.50	2448204.4582	09.10
2447956.3141	09.90	2448113.3900	09.90	2448204.4583	10.40
2447956.3884	09.90	2448113.8317	10.10	2448204.5328	09.80
2447956.3884	09.90	2448113.8317	09.90	2448215.2400	09.30
2447956.3886	10.00	2448113.8317	09.90	2448223.2300	09.70
2447956.4029	10.20	2448113.8317	09.70	2448231.2015	10.30
2447977.0079	10.10	2448113.8318	09.90	2448231.2400	09.80
2447977.0220	10.10	2448113.8460	09.80	2448231.3650	09.60
2447977.0220	09.80	2448113.8460	09.70	2448231.3791	10.10
2447977.0220	09.60	2448113.8462	10.40	2448231.3792	10.20
2447977.0220	09.60	2448113.9206	10.40	2448231.3792	09.30
2447977.0222	09.70	2448113.9207	10.80	2448231.3793	09.20
2447977.0966	09.10	2448124.3600	09.70	2448238.2400	09.40

HJD	V	HJD	V
2448255.6232	09.60	2448314.8052	09.20
2448255.6375	09.60	2448314.8194	09.30
2448255.7264	09.90	2448314.8194	09.30
2448255.8010	09.10	2448314.8194	09.30
2448255.8153	09.90	2448314.8194	09.70
2448261.2400	09.00	2448314.8196	09.50
2448297.3101	09.10	2448314.8941	09.60
2448297.4733	09.20	2448314.9083	10.20
2448297.4734	09.90	2448314.9083	09.50
2448297.4735	10.30	2448314.9084	09.10
2448297.4877	09.00	2448354.5246	09.50
2448297.4877	09.70	2448354.5246	09.10
2448297.4877	09.30	2448354.5246	09.40
2448297.4879	09.10	2448354.5247	10.40
2448297.5622	09.10	2448354.5389	09.00
2448297.5622	09.10	2448354.5389	09.10
2448297.5623	10.20	2448354.5389	09.80
2448297.5623	09.00	2448354.5389	10.20
2448297.5624	09.80	2448354.6136	09.40
2448297.5766	09.20	2448381.9831	10.30
2448297.5766	09.60	2448382.0718	09.40
2448297.5766	09.00	2448382.0719	09.20
2448297.5766	10.00	2448382.0719	09.30
2448297.5768	09.50	2448382.0720	09.90
2448297.6511	09.00	2448382.0863	09.60
2448297.6511	09.70	2448402.4600	09.00
2448297.6512	09.70	2448407.5754	09.80
2448297.6512	10.00	2448407.5754	09.30
2448297.6513	09.40	2448407.5755	10.00
2448297.6655	08.70	2448407.5897	10.20
2448297.6655	09.80	2448407.5898	09.30
2448297.6656	09.10	2448407.5899	09.90
2448297.7402	09.20	2448418.4000	10.20
2448297.7545	09.20	2448429.4500	09.60
2448314.4640	09.50	2448438.4800	09.70
2448314.5384	09.20	2448444.5471	10.10
2448314.5384	09.10	2448444.5471	09.20
2448314.5384	09.20	2448444.5472	09.60
2448314.5385	09.20	2448444.6216	09.70
2448314.5527	09.20	2448444.6216	10.10
2448314.5527	09.10	2448444.6217	10.20
2448314.5527	09.10	2448444.6218	09.50
2448314.5529	09.70	2448444.6359	10.30
2448314.6273	10.50	2448444.6360	10.20
2448314.6273	09.20	2448444.6362	09.70
2448314.6273	10.50	2448447.4600	10.00
2448314.6273	10.20	2448458.6646	09.80
2448314.6275	09.60		
2448314.6416	09.60		
2448314.6416	09.60		
2448314.6418	09.60		
2448314.8051	09.90		
2448314.8051	09.40		
2448314.8051	09.20		

Table 6.5: Photographic visual estimates collected by the author at Harvard Observatory

HJD	V
2439679.7390	09.10
2439732.5940	09.30
2439735.5930	09.30
2439738.5880	09.30
2440067.6760	08.50
2440417.7110	09.50
2440452.6220	09.70
2440774.7410	09.00
2440776.7350	09.35
2440824.6010	08.30
2442637.6550	09.30

---

# Chapter 7

## Bibliography

- Chevalier, R. A. 1981, *Fundamentals of Cosmic Physics*, 7, 1.
- Barthes, D., & Mattei, J. A. 1997, *Astronomical Journal*, 113, 373.
- Breger, M. 1993, *Astrophysics and Space Science*, 210, 173.
- Feast, M. W., Catchpole, R. M., Carter, B. S., & Roberts, G. 1980, *Monthly Notices of the Royal Astronomical Society*, 193, 377.
- Feast, M. W. 1984, *Proceedings of the Second Asian-Pacific Regional Meeting on Astronomy*, edited by B. Hidayat & M. W. Feast, p. 104.
- Fernie, J. D. 1963, *Astronomical Journal*, 68, 780.
- Fernie, J. D. 1989, *Publications of the Astronomical Society of the Pacific*, 101, 225.
- Flower, P. J. 1977, *Astronomy and Astrophysics*, 54, 31.
- Foster, G. 1996, *Astronomical Journal*, 111, 541.
- Glass, I. S. 1979, *Monthly Notices of the Royal Astronomical Society*, 186, 317.
- Guo, J. H., & Li, Y. 2002, *Astrophysical Journal*, 565, 559.
- Henden, A. A., 2006, *Observations from the AAVSO International Database*, private communication.
- Hertzsprung, E. 1928, *Bulletin of Astronomical Institutes of the Netherlands*, 4, 179.
- Hoffmeister, C., Richter, G., & Wenzel, W. 1985, *Variable Stars* (Springer-Verlag: Berlin).
- Humphreys, R. M. 1987, *Publications of the Astronomical Society of the Pacific*, 99, 5.
- Johnson, H. L. 1963, in *Basic Astronomical Data*, edited by K. A. Strand (University of Chicago Press: Chicago), p. 204.

- 
- Jurcevic, J. S., Pierce, M. J., & Jacoby, G. H. 2000, *Monthly Notices of the Royal Astronomical Society*, 313, 868.
  - Kholopov, P. N., Samus, N. N., Frolov, M. S., Goranskij, V. P., Gorynya, N. A., Kireeva, N. N., Kukarkina, N. P., Kurochkin, N. E., Medvedeva, G. I., Perova, N. B., & Shugarov, S. Yu. 1985, *General Catalogue of Variable Stars, Fourth Edition* (Nauka Publ. House: Moscow)
  - Kiss, L. L., Szatmary, K., Cadmus Jr., R. R., & Mattei, J. A. 1999, *Astronomy and Astrophysics*, 346, 542.
  - Kwee, K. K., & van Woerden, H. 1956, *Bulletin of the Astronomical Institutes of the Netherlands*, 12, 327.
  - Lee, T. A. 1970, *Astrophysical Journal*, 162, 217.
  - Li, Y., & Gong, Z. G. 1994, *Astronomy and Astrophysics*, 289, 449.
  - Meynet, G., Mermilliod, J. C., & Maeder, A. 1993, *Astronomy and Astrophysics Supplement Series*, 98, 477.
  - Mantegazza, L., Poretti, E., & Bossi, M., 1996, *Astronomy and Astrophysics*, 308, 847.
  - Mattei, J. A. 1993, *Journal of the American Association of Variable Star Observers*, 22, 47.
  - Mattei, J. A., & Foster, G. 2000, In *Variable Stars as Essential Astrophysical Tools*, edited by C. Ibanoglu (Dordrecht: Boston), NATO Science Series, Series C, Mathematical and Physical Sciences, Vol. 544, p. 485.
  - Mattei, J. A., Foster, G., Hurwitz, L. A., Malatesta, K. H., Willson, L. A., & Mennessier, M. O. 1997, In *Proceedings of the ESA Symposium 'Hipparcos - Venice '97'*, ESA SP-402, p. 269.
  - Monnier, J. D., Geballe, T. R., & Danchi, W. C. 1998, *Astrophysical Journal*, 502, 833.
  - Pierce, M. J., Jurcevic, J. S., & Crabtree, D. 2000, *Monthly Notices of the Royal Astronomical Society*, 313, 271.
  - Press, W. H., Teukolsky, S. A., Vetterling, W. T., & Flannery, B. P. 1992, *Numerical Recipes in C: The Art of Scientific Computing, 2nd Edition* (Cambridge University Press: Cambridge).

- 
- Schaller, G., Schaerer, D., Meynet, G., & Maeder, A. 1992, *Astronomy and Astrophysics Supplement Series*, 96, 269.
  - Schrijver, C. J., & Pols, O. R. 1993, *Astronomy and Astrophysics*, 278, 51.
  - Sharpless, S., Riegel, K., & Williams, J. O. 1966, *Journal of the Royal Astronomical Society of Canada*, 60, 15.
  - Stothers, R. 1969a, *Astrophysical Journal*, 155, 935.
  - Stothers, R. 1969b, *Astrophysical Journal*, 156, 541.
  - Turner, D. G., & Forbes, D. 1982, *Publications of the Astronomical Society of the Pacific*, 94, 789.
  - Turner, D. G. 2006, *Odessa Astronomical Publications*, 18, in press.
  - Wood, P. R., & Bessell, M. S. 1985, *Publications of the Astronomical Society of the Pacific*, 97, 681.

---

## Vita

Name: Mina Rohanizadegan

Place of Birth: Tehran, Iran

Education: University of Tehran  
Tehran, Iran  
2003 B. Sc. in Physics

Saint Mary's University  
Halifax, Nova Scotia  
2006 M. Sc. in Astronomy

Related Experience: Guest Observer  
Harvard College Observatory Photographic Plate Stacks  
May 2005

Publications:

Rohanizadegan, M., Turner, D. G., Pastukhova, E. N., and Berdnikov, L. N. "The Origin of Brightness Variations in BC Cygni," *Journal of the Royal Astronomical Society of Canada*, 99, 143, 2005. (abstract)

Rohanizadegan, M., Turner, D. G., Pastukhova, E. N., and Berdnikov, L. N. "The Origin of Brightness Variations in BC Cygni," *Odessa Astronomical Publications*, 18, in press, 2006.



**Saint Mary's  
University**

Halifax, Nova Scotia  
Canada B3H 3C3

Patrick Power Library

tel 902.420.5534

fax 902.420.5561

web [www.stmarys.ca](http://www.stmarys.ca)

## **Copyright Permission Notice**

Documentation regarding permissions for the use of copyrighted material in this thesis is on file at the Saint Mary's University Archives. Contact us if you wish to view this documentation:

Saint Mary's University, Archives  
Patrick Power Library  
Halifax, NS  
B3H 3C3

Email: [archives@smu.ca](mailto:archives@smu.ca)  
Phone: 902-420-5508  
Fax: 902-420-5561

w h e r e   t r a d i t i o n   m e e t s   t h e   f u t u r e